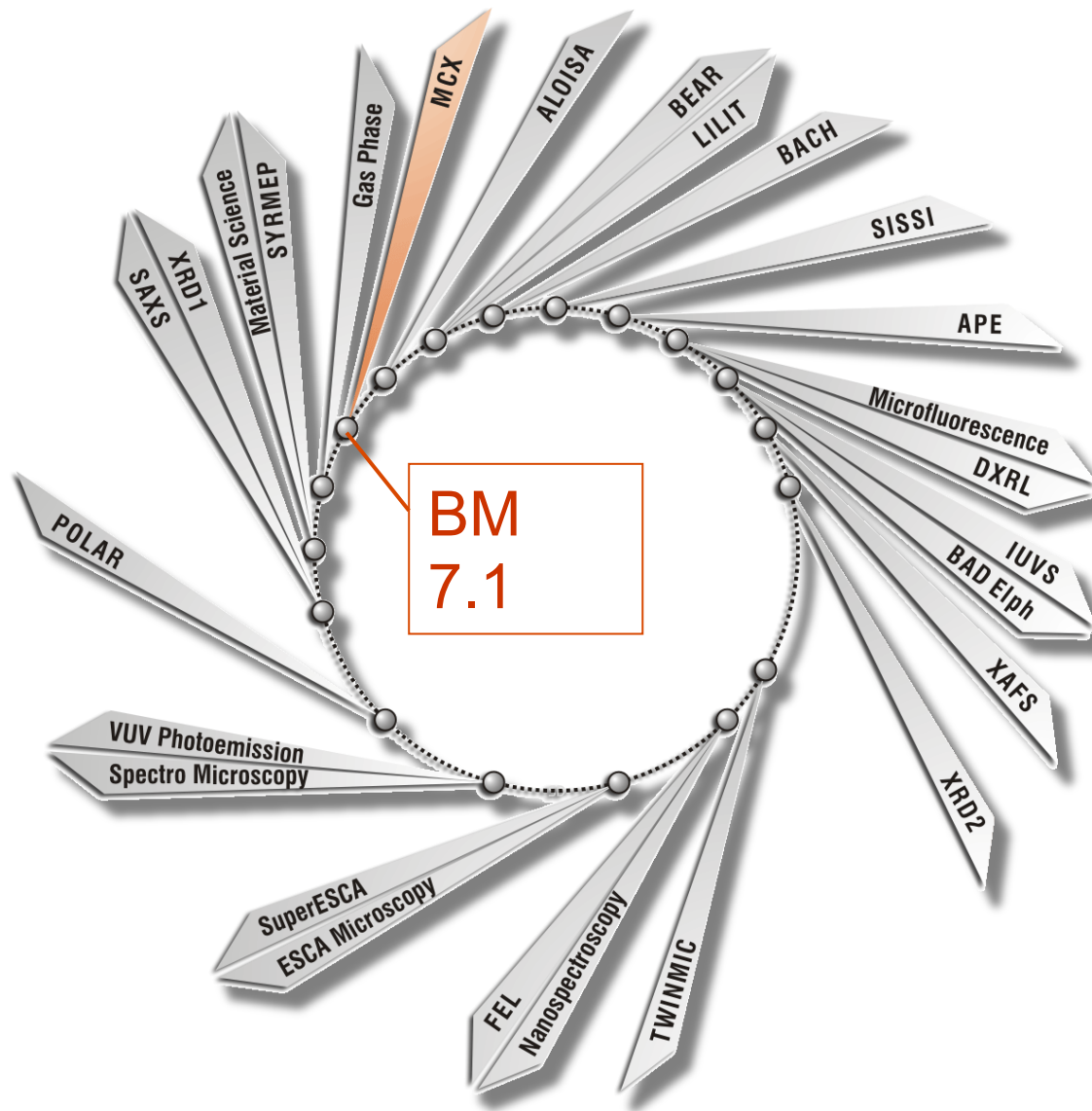


Diffraction at ELETTRA



2009 - Present:

MCX

new XRD1

currently in
construction:

XRD2



MCX focus

- Powder diffraction
- Powder diffraction in non-ambient conditions
- Anomalous resonant scattering
- Stress and Texture Analysis
- X-ray Reflectivity
- Grazing angle diffraction and reflectivity
 - organic and inorganic thin films
 - thermally and/or mechanically modified surfaces of mechanic components
 - polymers
 - catalysts
 - highly disordered materials in the form of:
 - films, powders, fibres

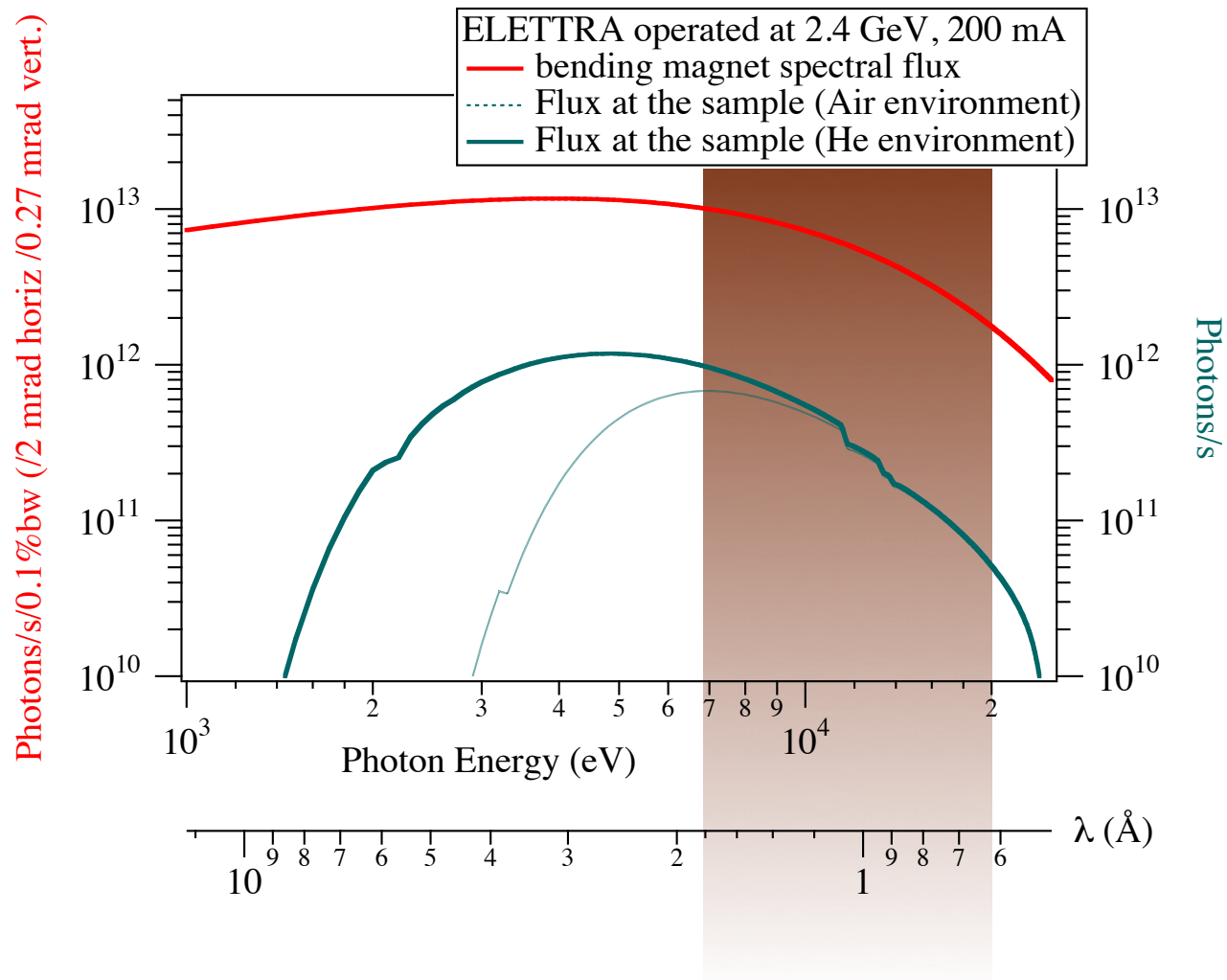


Design Guidelines

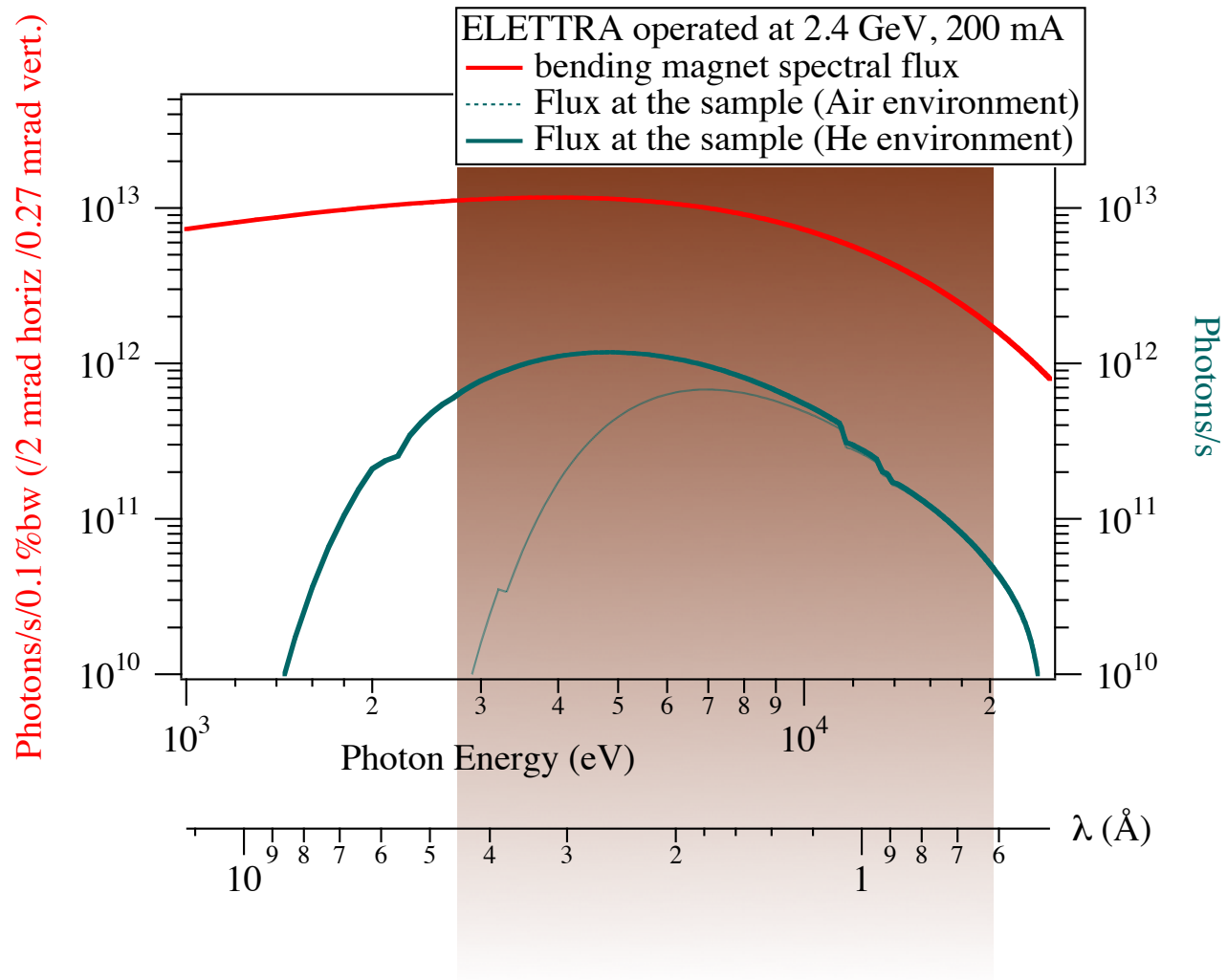
- High-flux tuneable source with a wide spectral range, (4-20 keV) Fe K-edge to Mo K-edge at least
[2.3 - 23 keV]
- Flexible optics
 - line focus (10 x 1 mm²) [4 x 0.3]
 - point focus (1 x 1 mm² and below) [0.3 x 0.3]
- Accommodate large volume samples)
[150 x 150 x 50 mm³ - 5kg]
- Use of different detectors
 - Counters, 1-D, area
- User-friendly software



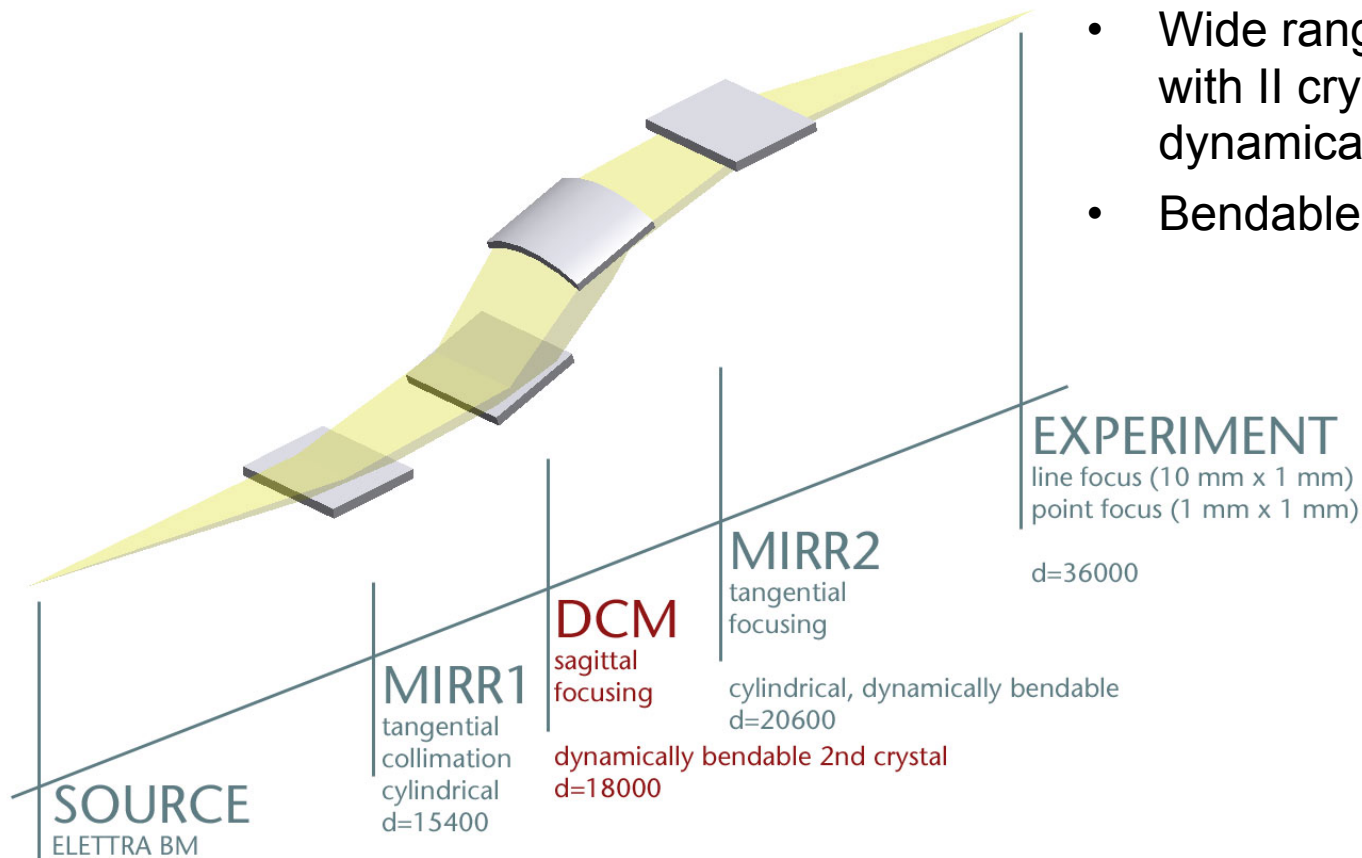
MCX optical design



MCX optical design



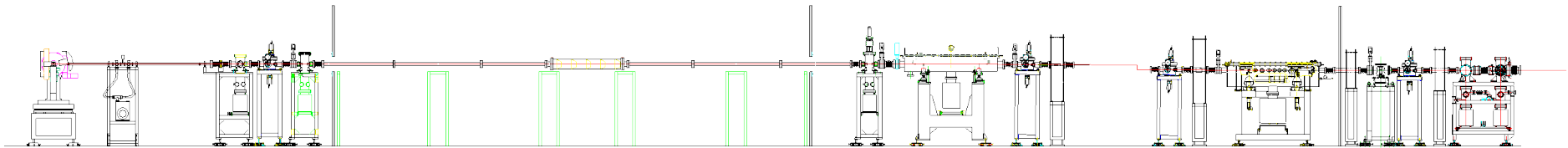
MCX optical design



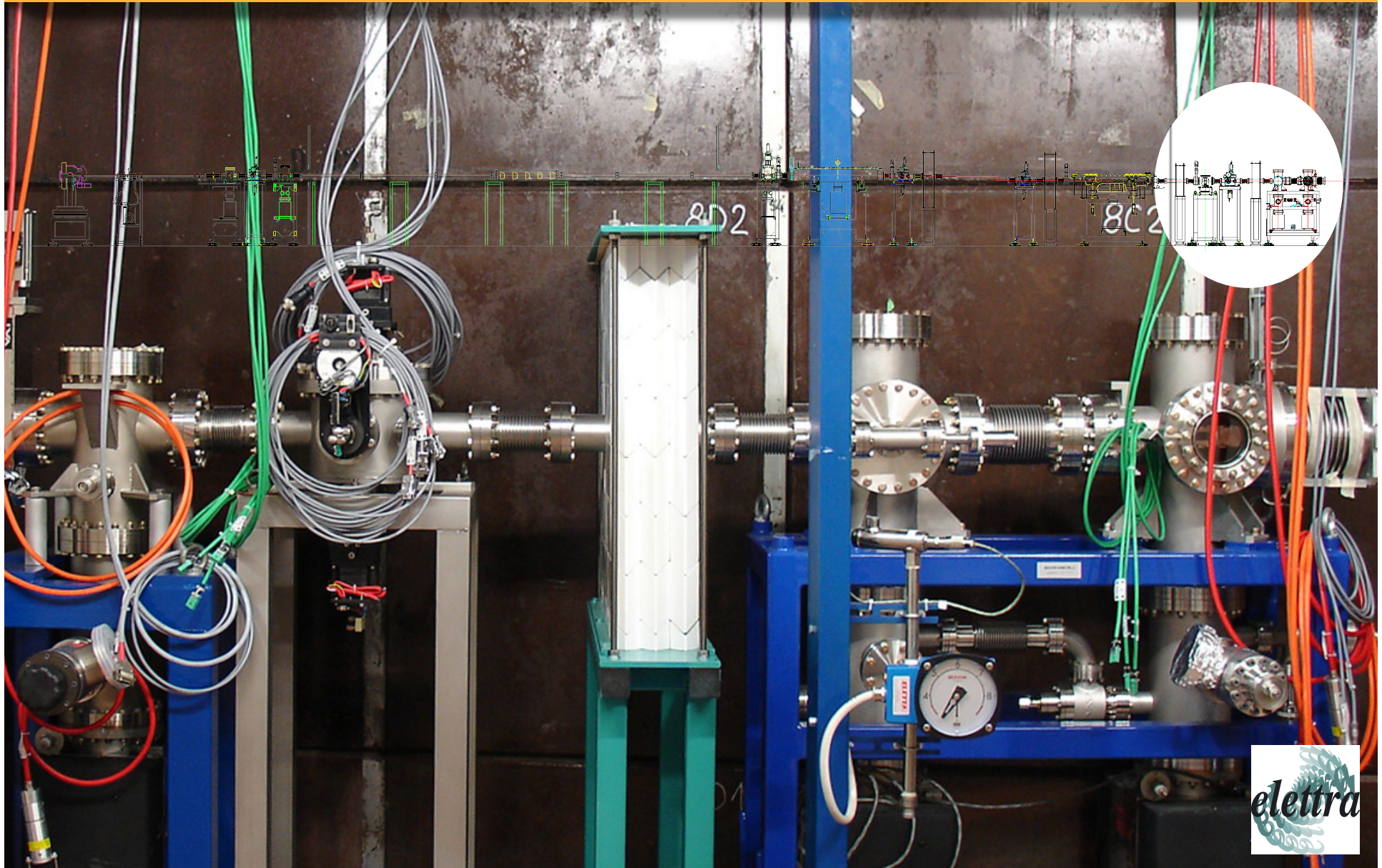
- High-transmission Filter-window assembly
- Collimating Pre-mirror
- Wide range monochromator with II crystal bender for dynamical sagittal focusing
- Bendable focusing mirror



18 + 18 mt...



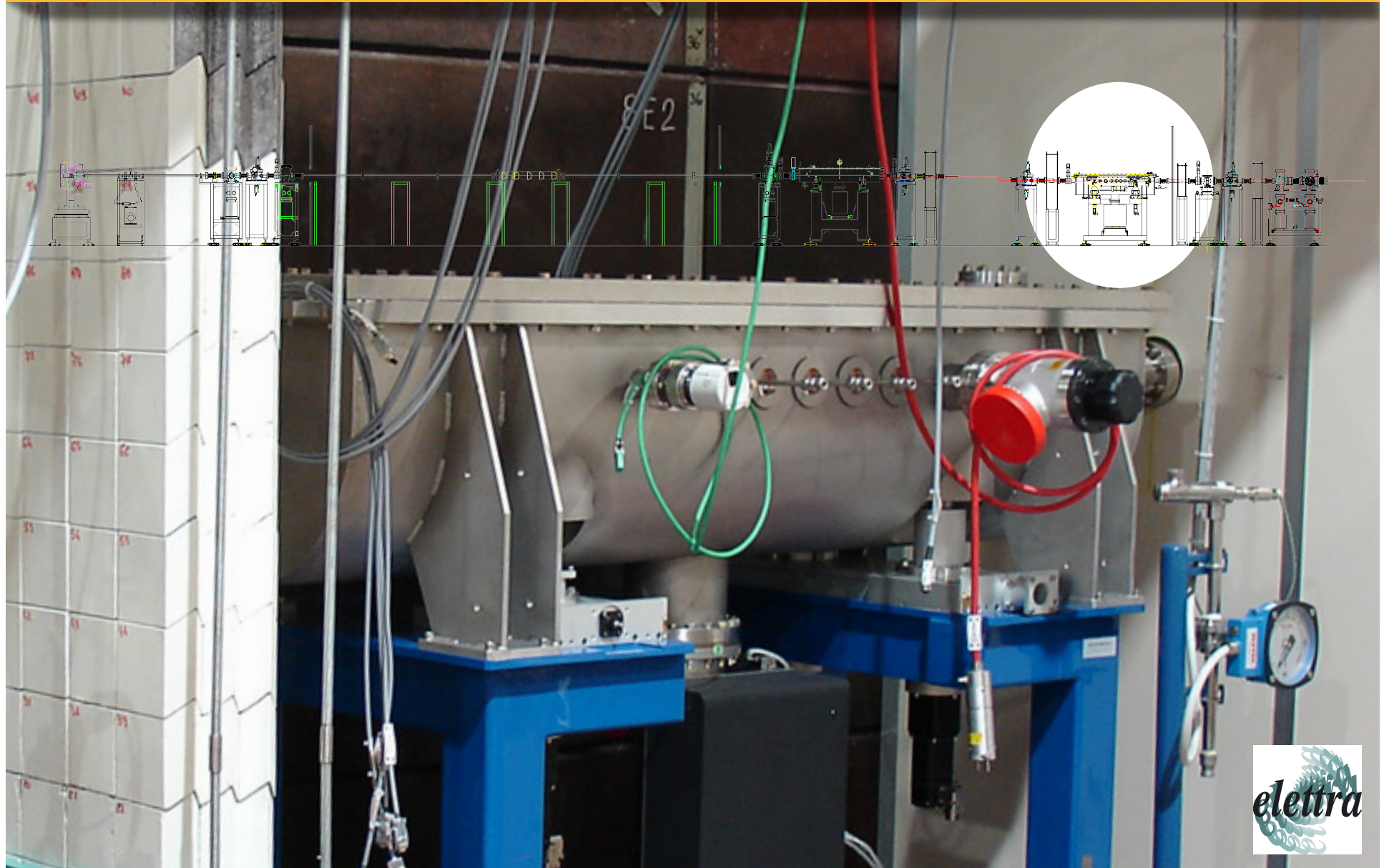
Front-End Hutch



Andrea Lausi The MCX beamline



Optical Hutch



Andrea Lausi The MCX beamline



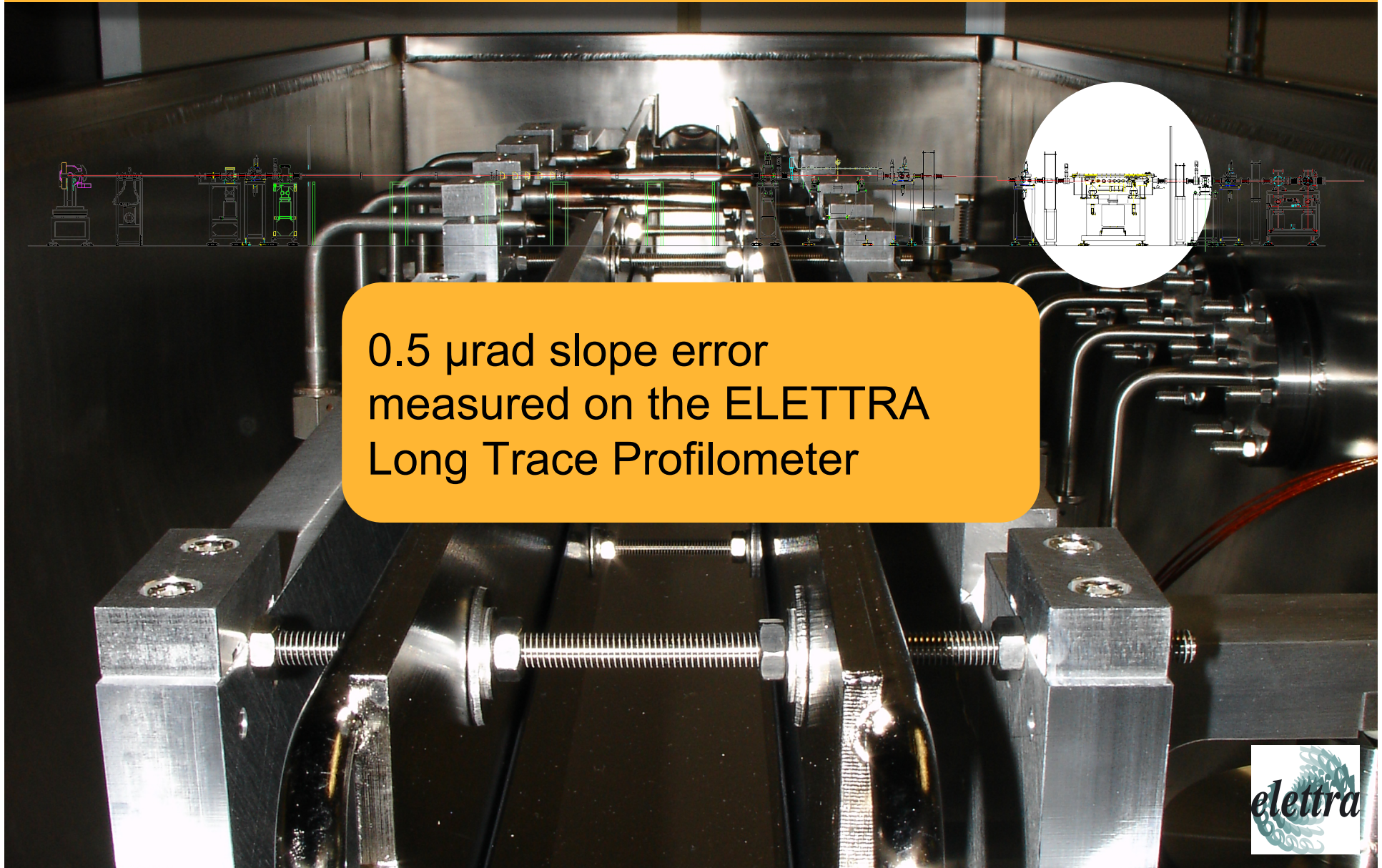
Optical Hutch



Andrea Lausi The MCX beamline



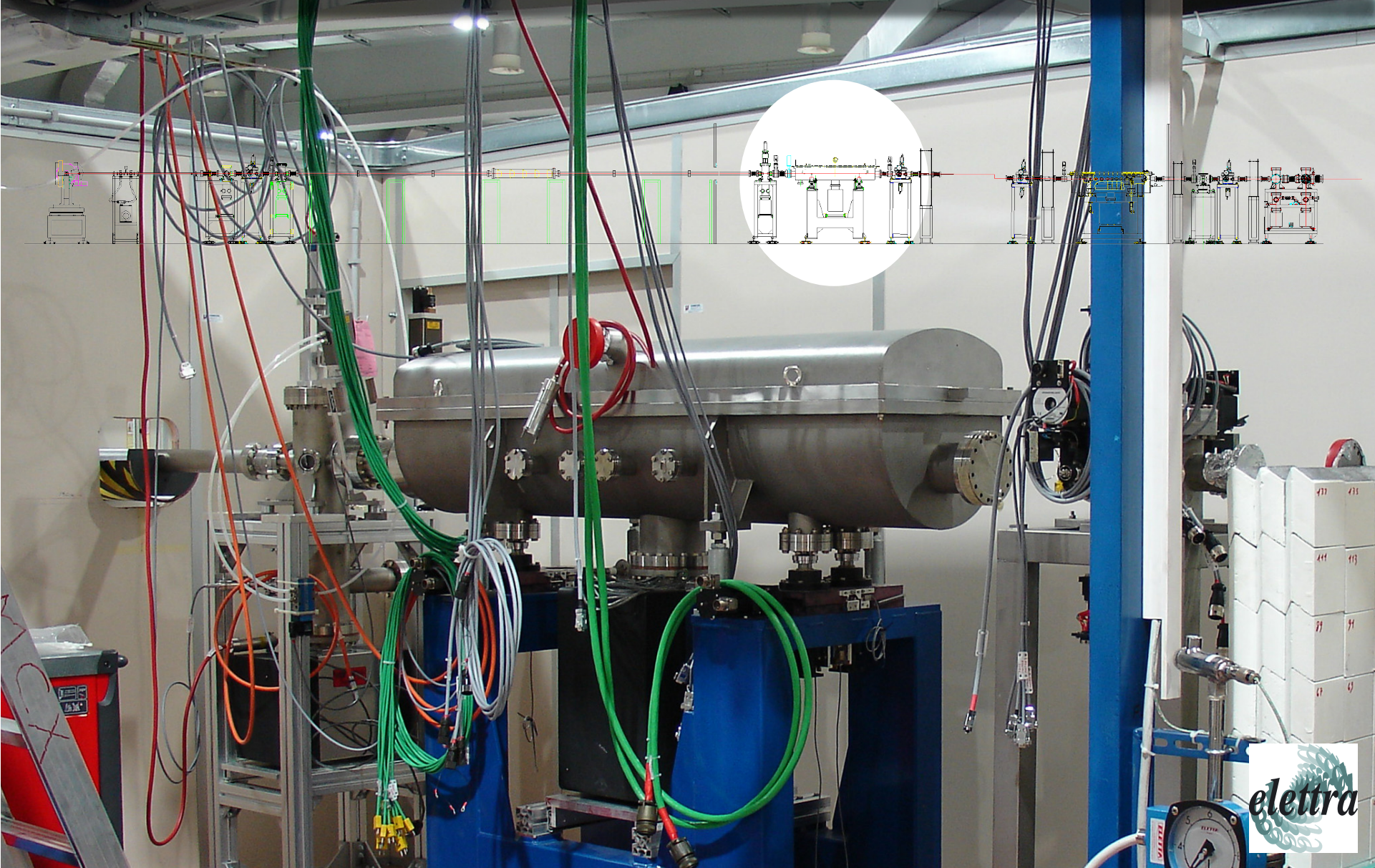
Optical Hutch



0.5 μ rad slope error
measured on the ELETTRA
Long Trace Profilometer



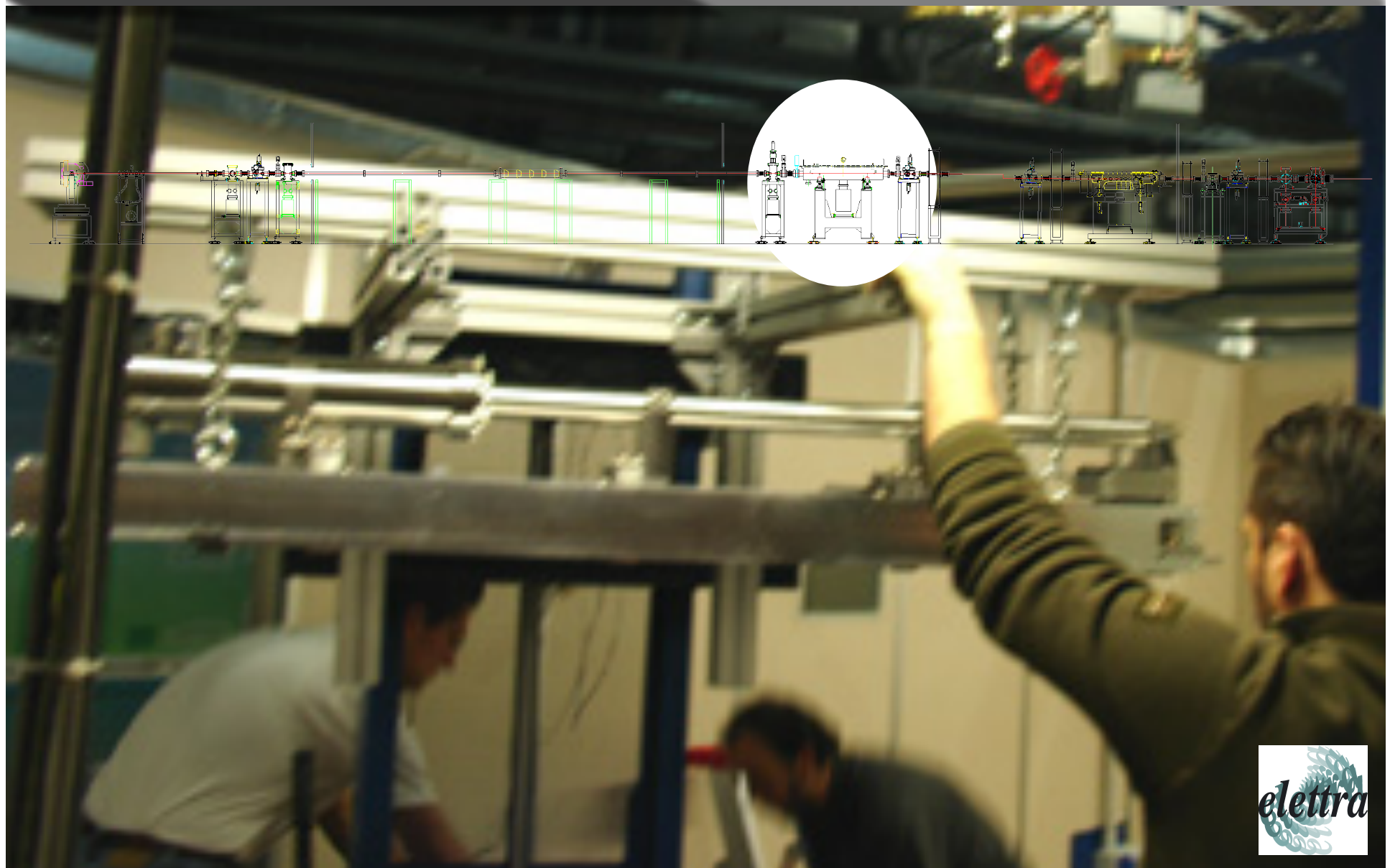
Optical Hutch



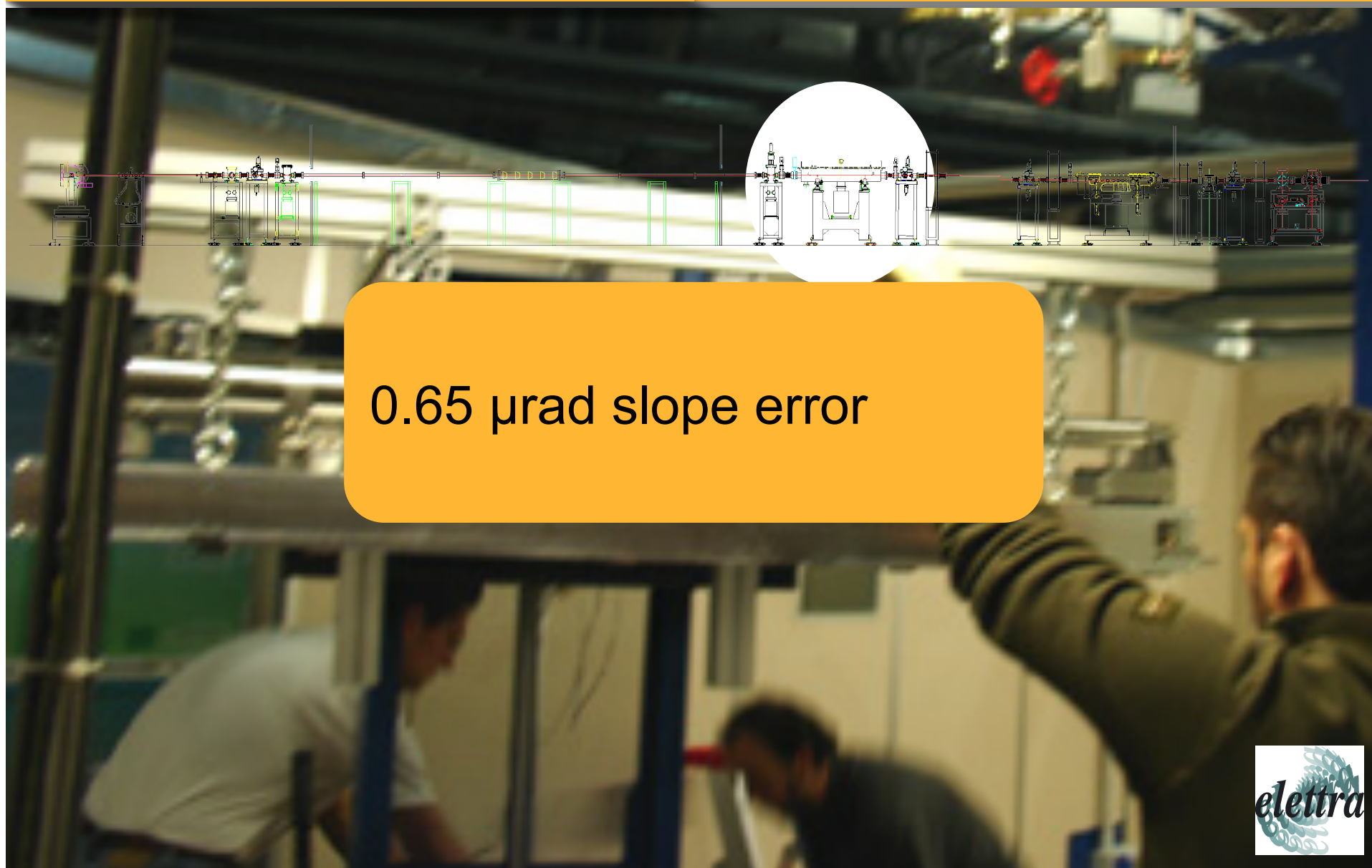
Andrea Lausi The MCX beamline



Optical Hutch



Optical Hutch



0.65 μ rad slope error

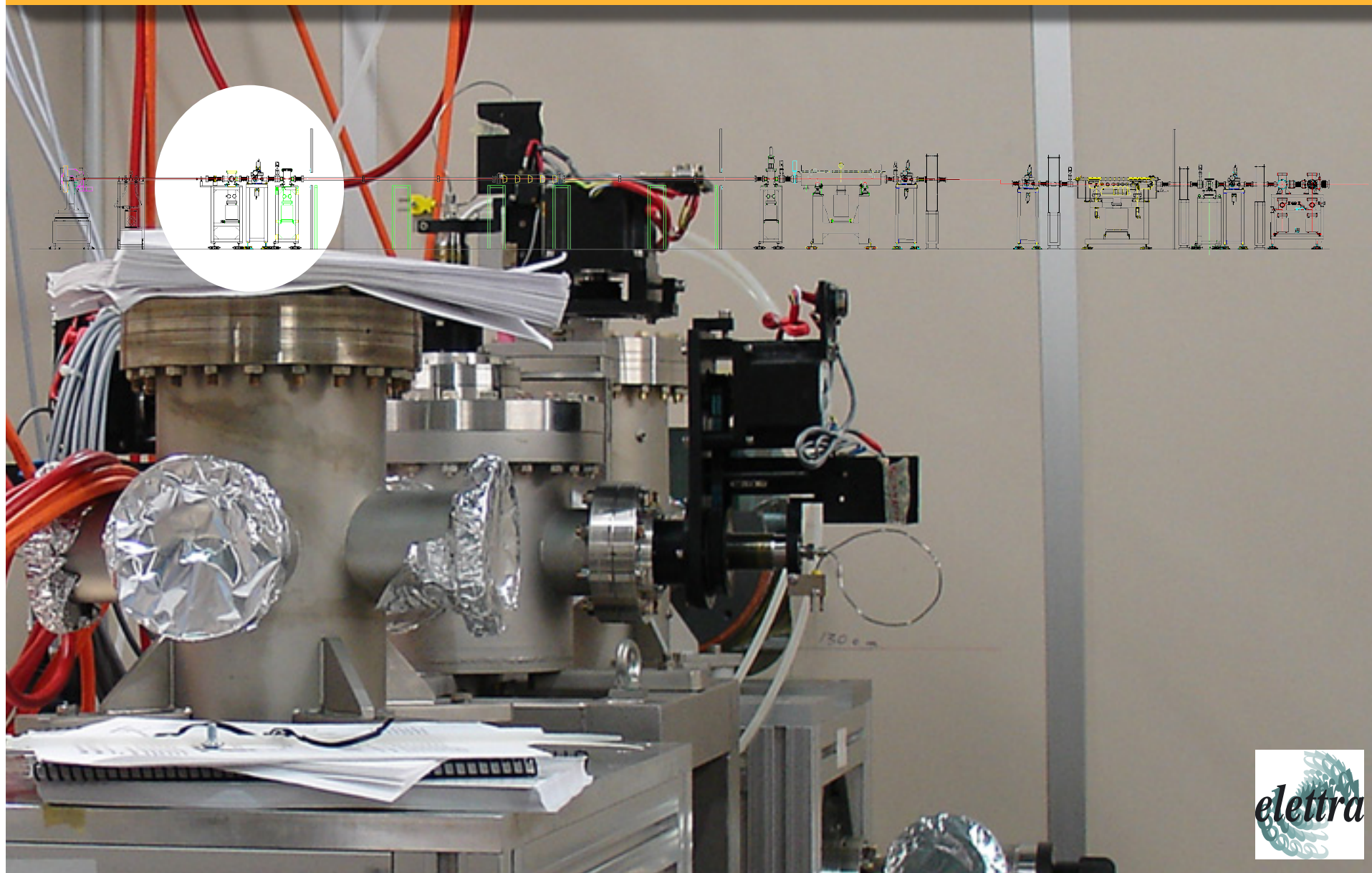


from the Optical Hutch to the Experimental Station

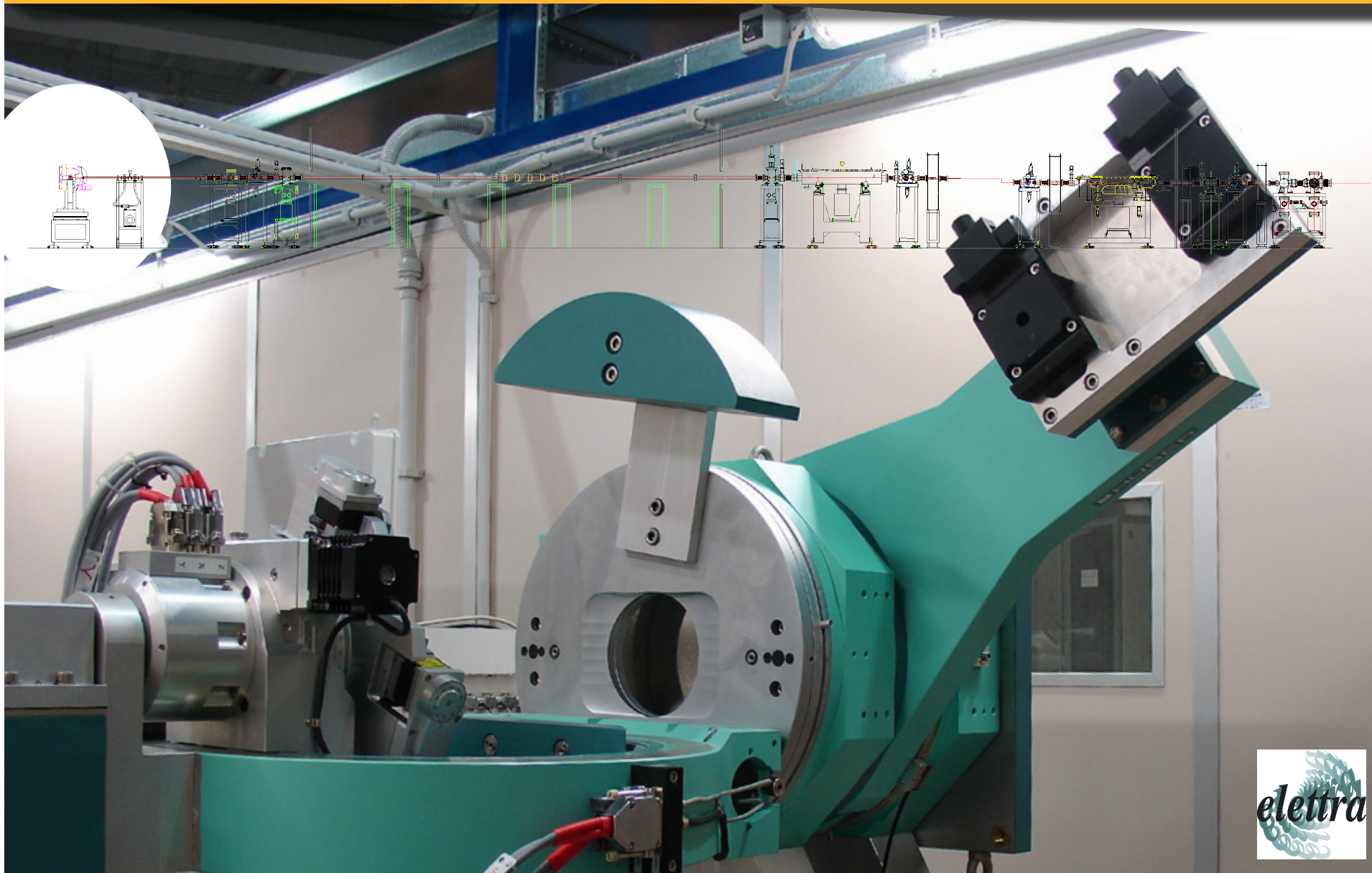


Andrea Lausi The MCX beamline

Experimental Station

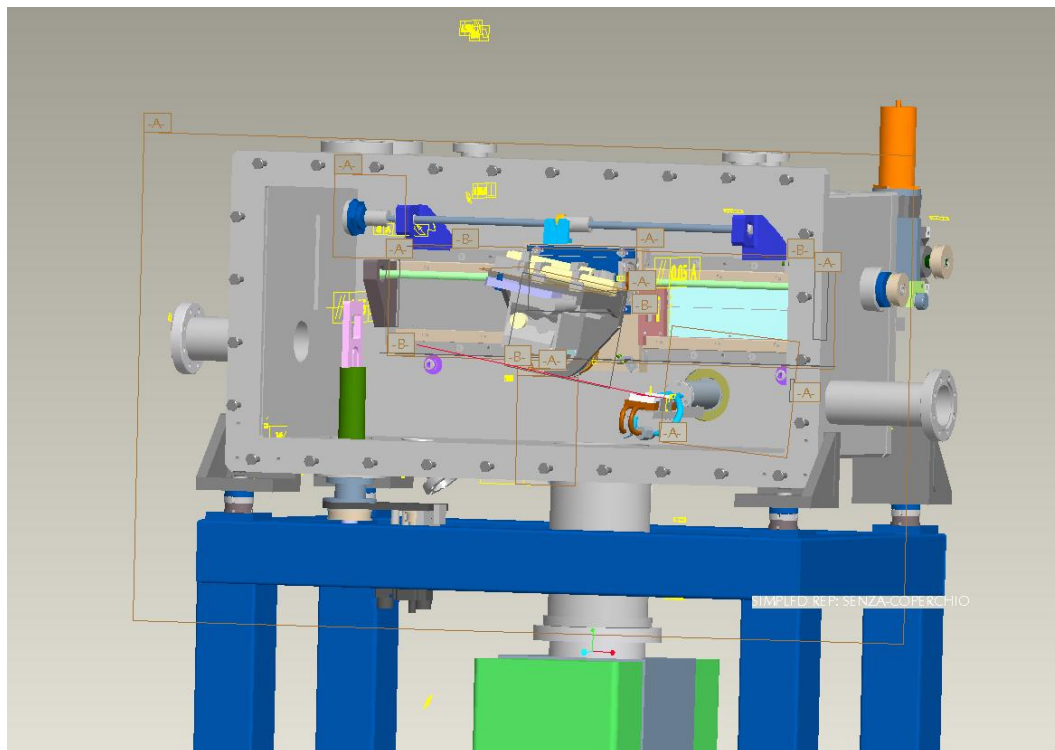


Experimental Station



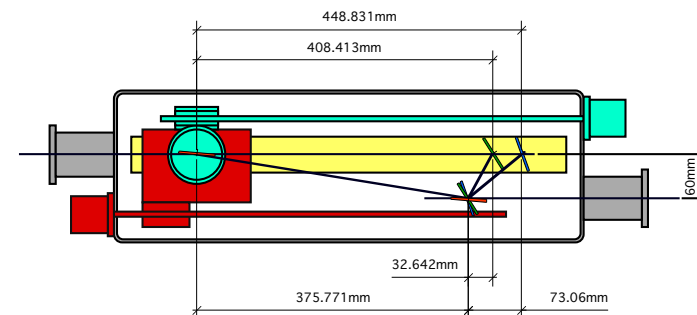
Andrea Lausi The MCX beamline

The ELETTRA Hard X-ray Monochromator



E. Busetto, I. Cudin, G. Fava
R. Borghes, G. Causero
A. Lausi, G. Zeraushek

X-ray monochromator: conceptual layout

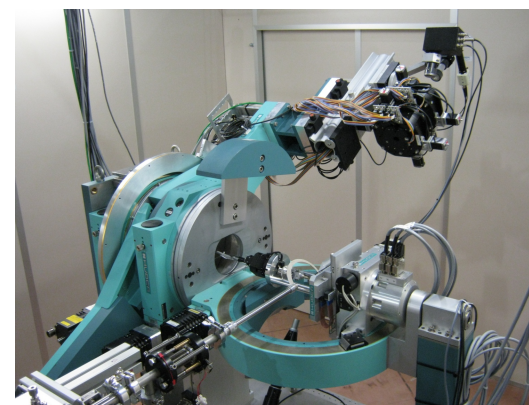
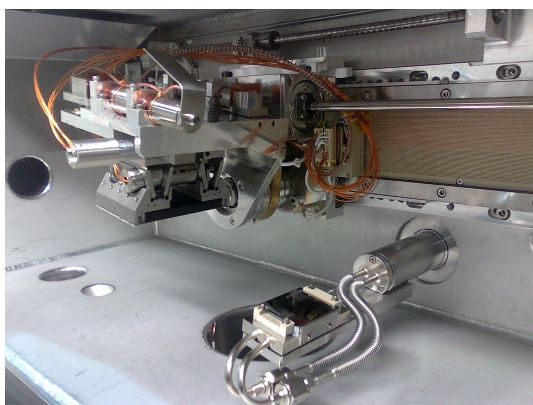


Si(111)
crystal positions: ■ 2100 eV $\theta = 70.3^\circ$ ■ II crystal translation
■ 2300 eV $\theta = 59.3^\circ$ ■ II crystal rotation
■ 25000 eV $\theta = 4.5^\circ$ ■ slide rail

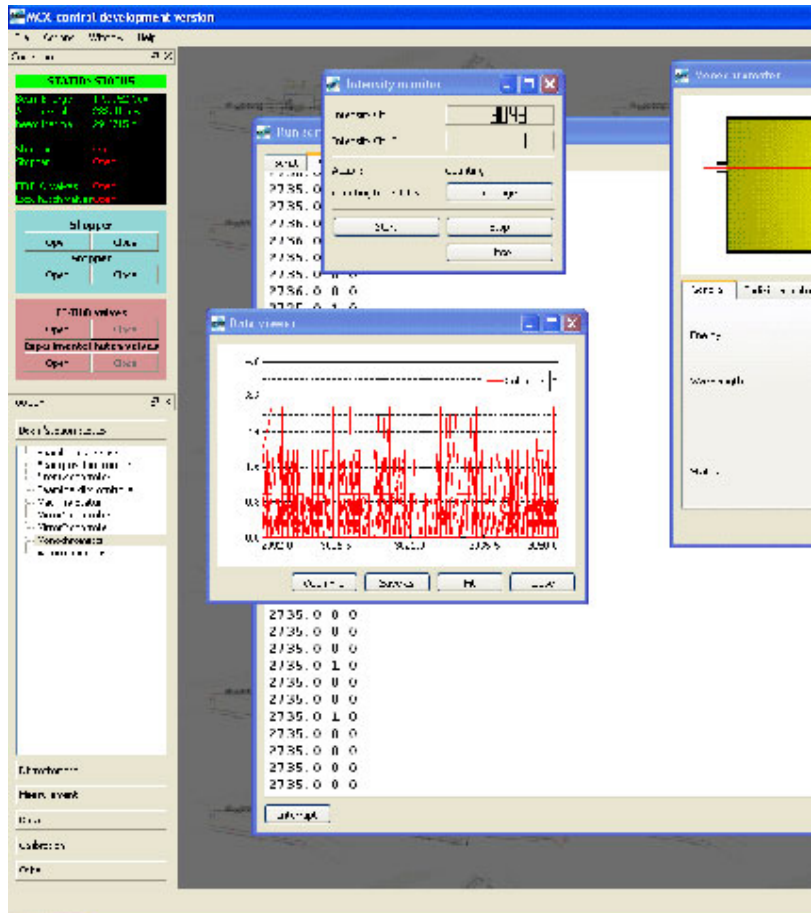
long 2nd crystal movement
capability allow for the
wide energy range



Commissioning the new beamline



Providing the user interface



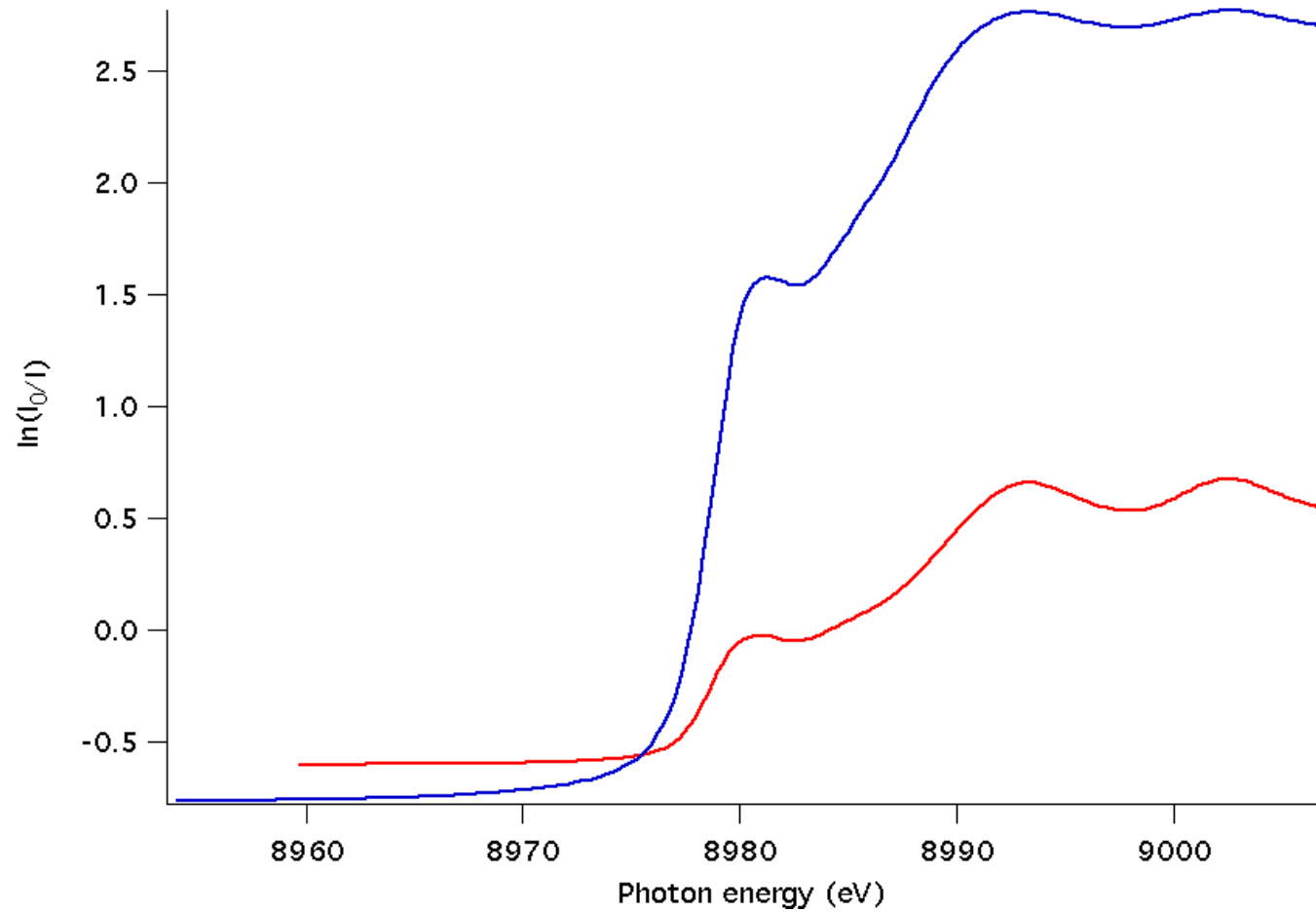
Control system based on python

General command interface for:

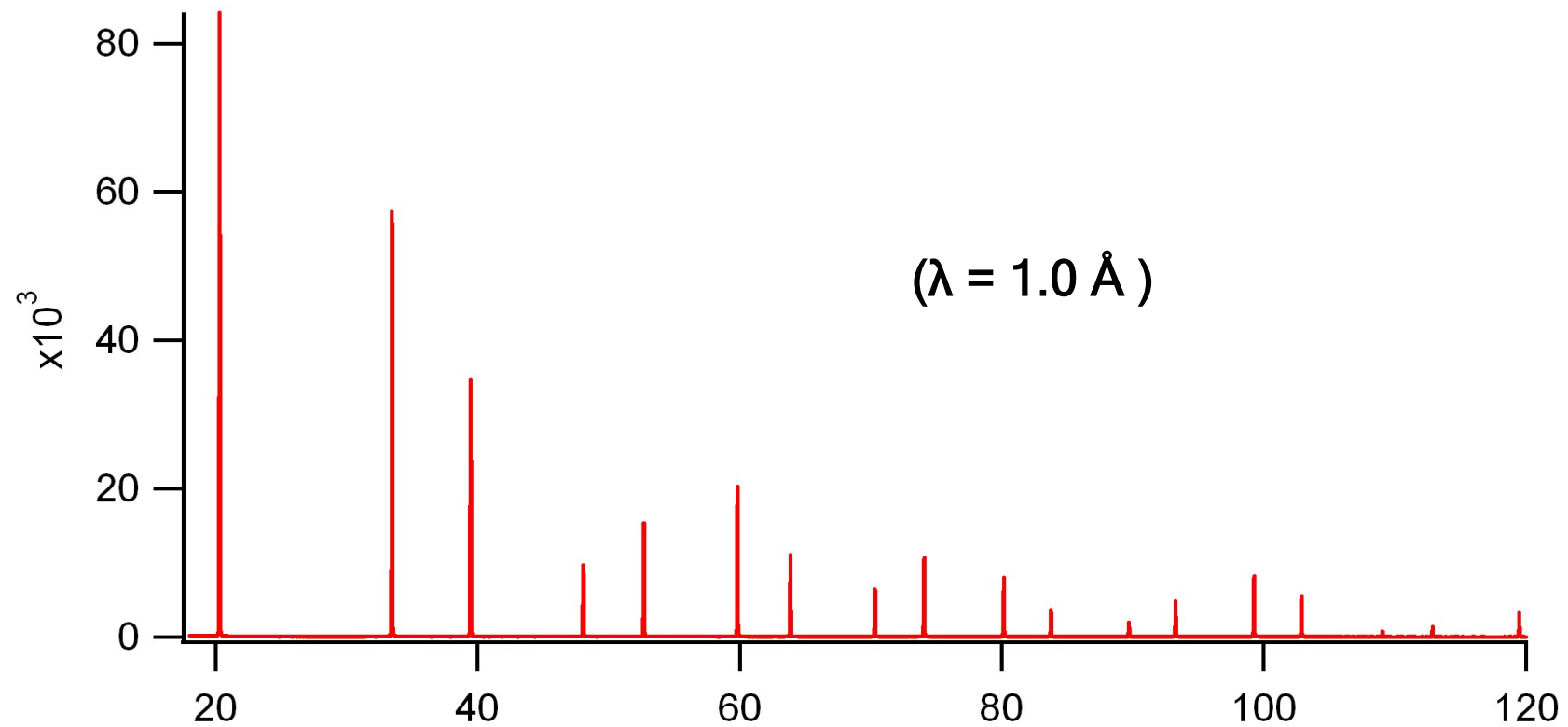
- driving motors
- theta-2theta scan
- multiple theta-2theta scans
- single or two motor scan
- multiple scans
- monochromator functions
- calibration functions
- warnings management...
- ...



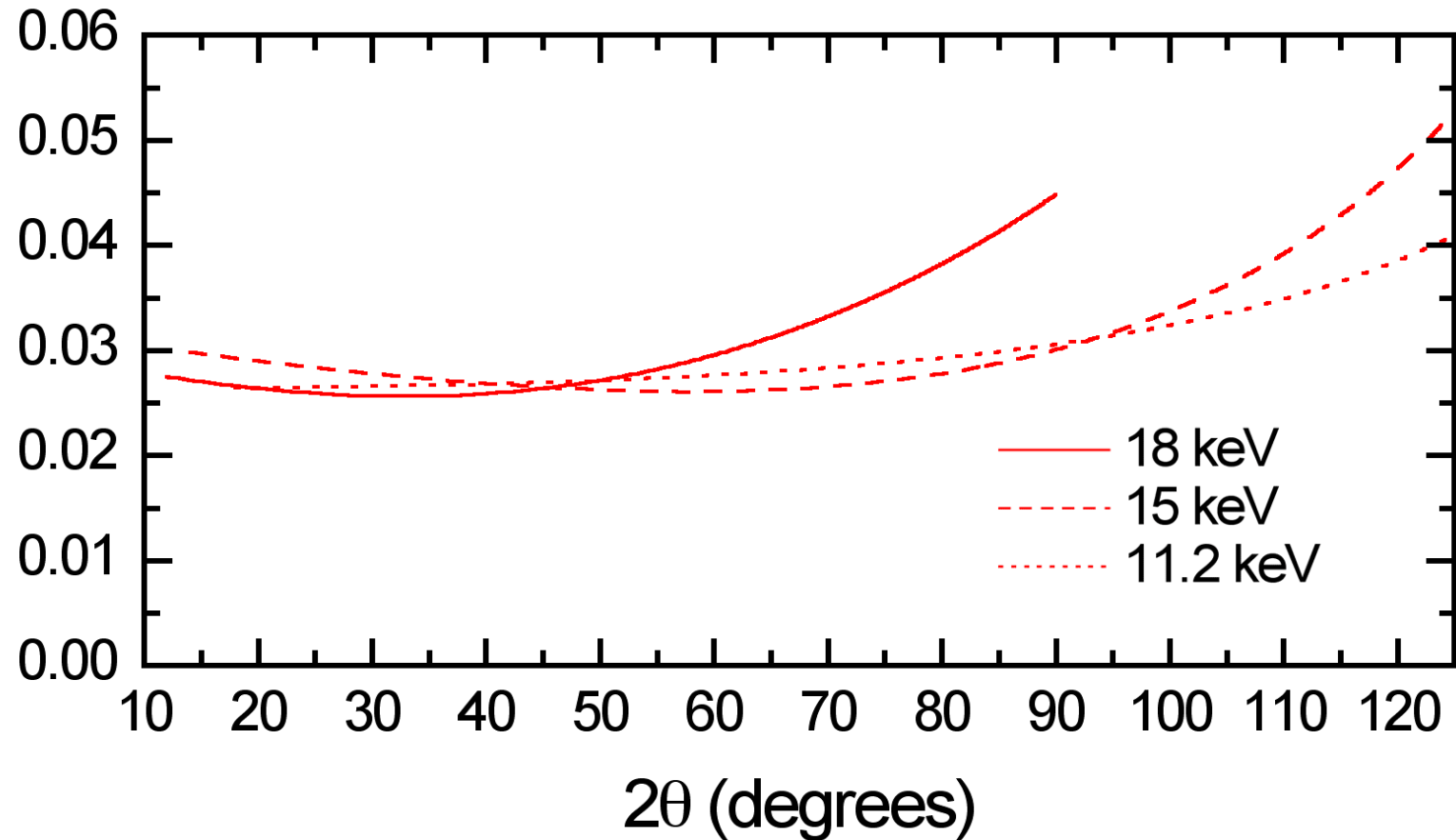
“tuning” the first mirror



Si powder test run



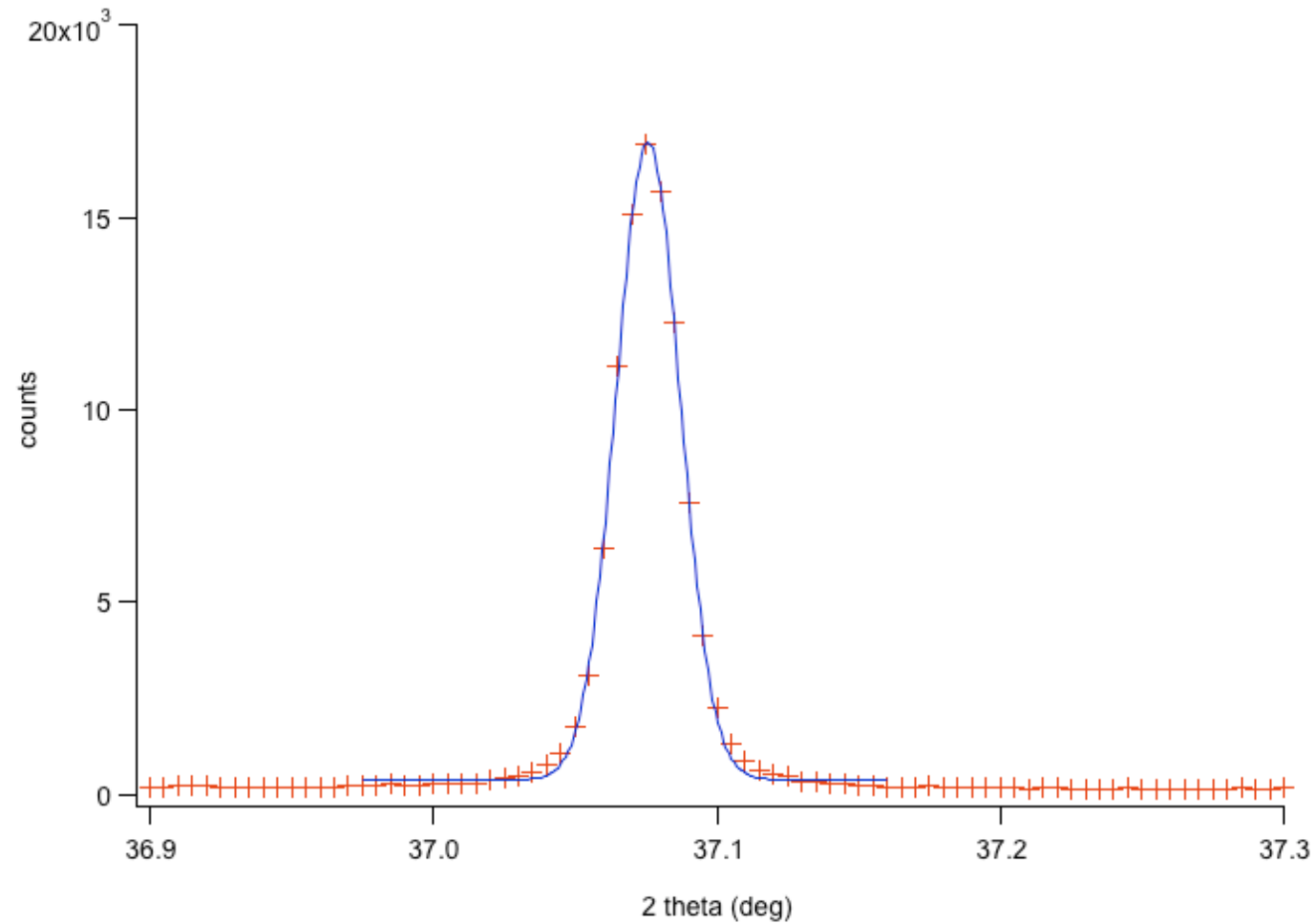
Si powder test run



FWHM of diffraction peaks of Si at various energies



Si powder test run



Negligible asymmetry in the instrumental broadening !



X-ray detectors

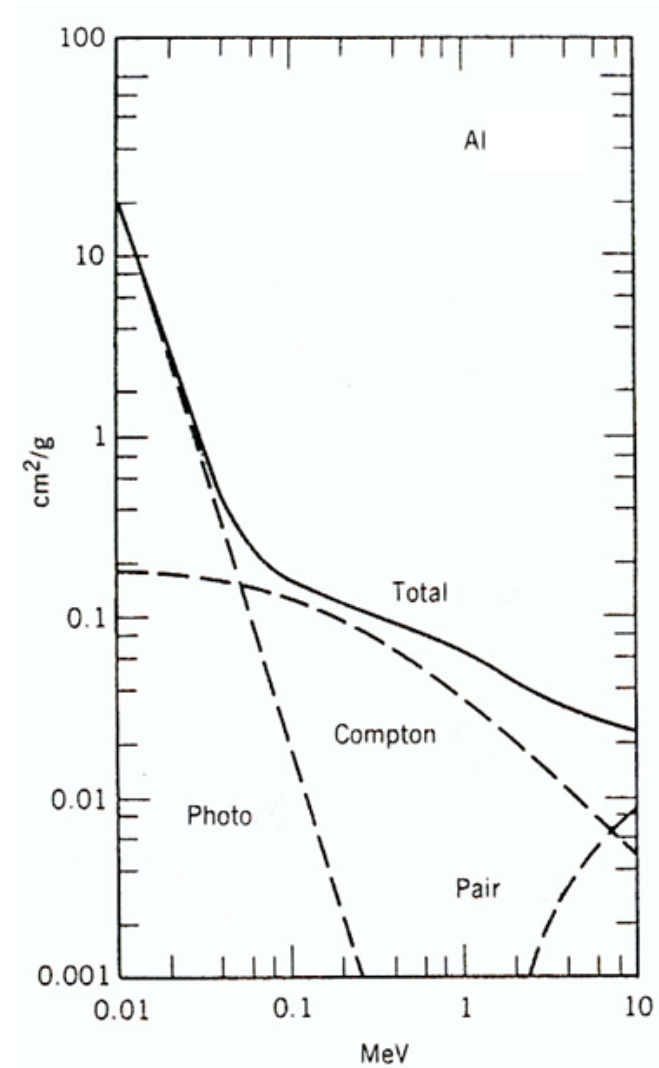
$$I(x) = I_0 e^{-\mu x}$$

□ Photon is absorbed (photoelectric effect) and energy is transferred to an electron

- Heat
- Fluorescence
- Ionization
- Creation of defects in a crystal
- Electron-hole pairs in a semiconductor

□ Compton Effect

□ Pair Creation above 1022 keV



General classification

A. COUNTERS

- “ALL” electrons produced during absorption of a SINGLE photon are collected.
- The signal is proportional to the absorbed energy.
 - gas proportional counters
 - Scintillation detectors
 - solid state detectors (including direct illumination CCDs)
 -

B INTEGRATORS

- charge collected is integrated over all absorption events, any correlation with the energy of each absorbed photon is lost.
- The signal is proportional to the number of absorbed photons.
 - film
 - Imaging Plate
 - various CCD-based systems
 -



properties

- Quantum efficiency
- Time properties
 - Dinamic Range
 - Linearity
 - Count rate
- Spatial properties
 - resolution
 - uniformity
 - distorstions
- Energy resolution
- Data flux
- dimensions, weight and reliability
- costs



Statistics and noise

- The efficiency of the detection is determined both by the absorption efficiency and by the noise level. *Shot noise* represents the ultimate limit in the photon detection process.

$$\bar{x} = N$$

$$\sigma = \sqrt{N} \quad \bullet(\text{shot noise})$$

- An ideal detector is than an apparatus which has, in experimental conditions, an intrinsic noise level smaller than the *shot noise*, and this consideration is at the origin of the factor of merit known as Detective Quantum Efficiency:

$$\text{DQE} = \frac{(S_o/N_o)^2}{(S_i/N_i)^2}$$



Statistics and noise

- In an ideal detector all absorbed photons contribute effectively to the output signal, and no other source of noise is present

$$\left(S_i/N_i\right)^2 = N \qquad \left(S_o/N_o\right)^2 = \alpha N$$

- so that the DQE of an ideal detector is simply equal to its absorption coefficient α , over the entire range of input intensities.

- suppose to require a measure with an accuracy ρ it is then easy to obtain
- that for a source with a fixed number N of photons per unit time the time t needed is given by:

$$t = \frac{1}{N \cdot \text{DQE} \cdot \rho^2} = \frac{1}{N\alpha\rho^2}$$

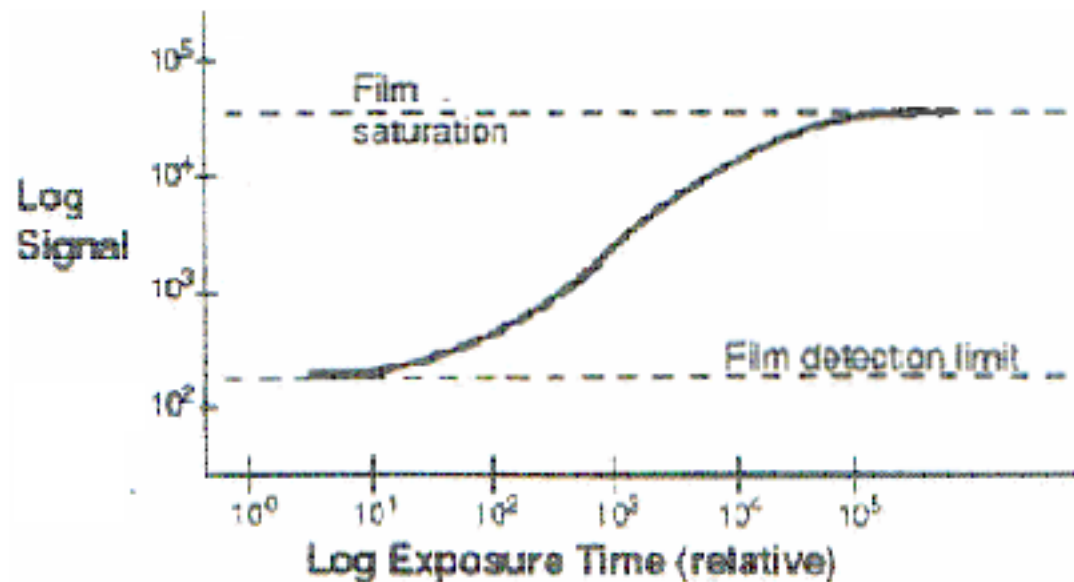


Count rate, dynamic range and linearity

- minimum and maximum number of events per unit time

$$\text{Dynamic Range} = \frac{\text{maximum measurable level}}{\text{noise level in absence of input signal}}$$

- Alternatively, the dynamic range can be defined as the range of input signal intensity for which the DQE exceeds a given value. Actually, this second definition for the dynamic range, taking into account the effects of the input signal, gives a better description of the behaviour of a detector in working condition, which can be affected by e.g. the spatial response of the instrument



Spatial properties

- The MTF is given by the ratio between the intensity variation in the image and the intensity variation in the object, as a function of the spatial frequency.

$$\text{MTF}(k) = \frac{I_o(k)}{I_i(k)}$$

- The advantage of the MTF in analysing a detector system is that the MTF of a cascade of series elements is simply the product of the MTF of each element.

$$\text{MTF}_{1,2,\dots,N}(k) = \text{MTF}_1(k) \cdot \text{MTF}_2(k) \cdot \dots \cdot \text{MTF}_N(k)$$

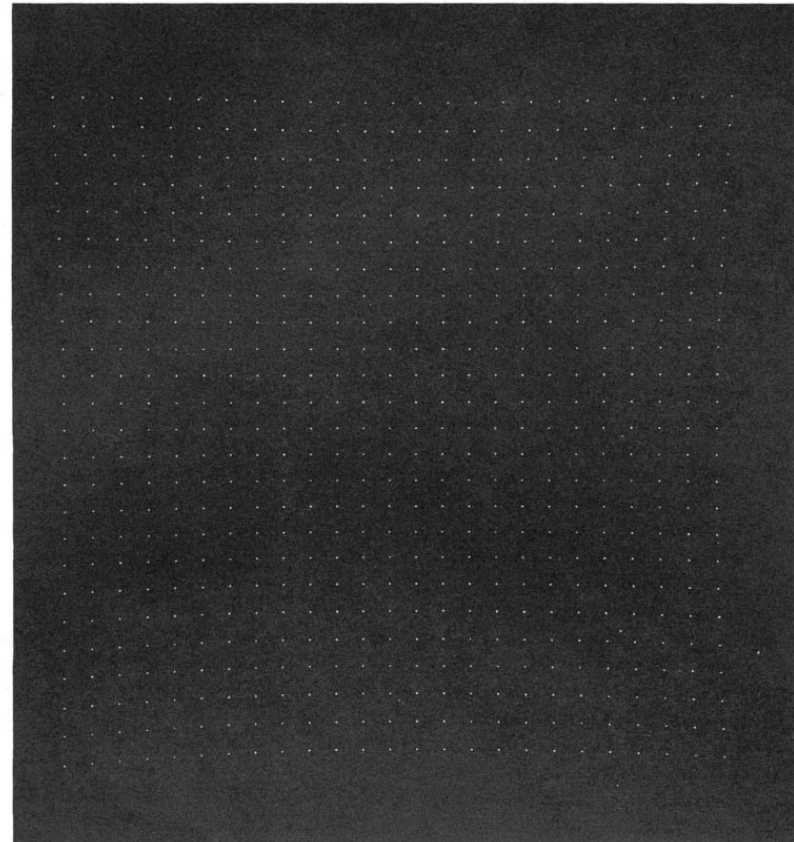
$$\text{PSF} = \text{F}(\text{MTF})$$

$$\text{Spatial Resolution} = \text{FWHM} (\text{PSF})$$



Spatial properties

•The uniformity of response is also an important requisite of an area detector. This is in general not a problem for photographic film but, to a certain extent, all position sensitive electronic detectors show both long and short range variations of response. Low spatial frequency distortions can be easily corrected by using smooth functions. Calibration of high spatial frequency variation (pixel-to-pixel non-uniformity) is instead usually performed by providing a smooth and constant flat field illumination across the whole detector area. Moreover these fluctuations are in general dependent on the energy deposited in the detector, i.e. on the energy of the incoming photons. For use at a synchrotron source, where the photon energy spectrum is wide, the calibration of such a detector becomes consequently a delicate and time-consuming procedure.



Energy discrimination

- In general:

$$\Delta E_{FWHM} = 2.35 \sqrt{F \cdot E_i \cdot E_{event}}$$

- E_i energy of the absorbed photon
- E_{event} energy spent in the absorption process
- F empiric factor (by U. Fano)

$$F = \left(\frac{\text{resoluzion observed}}{\text{resolution expected for pure Poisson statistics}} \right)^2$$

- $F \sim 0.1$ in a semiconductor and 0.2 in a gas
- $E_{event} = 26$ eV noble gas
- $E_{event} = 3.6$ eV Si @ 300 K



Data handling

- When area detector are concerned, data analysis and storage are as important factors as the acquisition itself, and should be considered as one of the main features of the instrument. To give an idea of the dimension of the problem, it is enough to consider that a 1000x1000 pixel image with a dynamic range of 16 bit gives already 2 Mbytes/frame. The problem may extend then also to data transfer if time resolution requires fast framing.



Latent image detectors: Photographic film

The image is formed by the reduction of AgBr into metallic Ag grains during the chemical development. The blackening, expressed in optical density units D , is then read with a microdensitometer measuring the ratio between the light transmitted and incident onto the film:

$$D = -\log_{10}(I_{trasmessa} / I_{incidente})$$

The values of D are limited to the interval 0.1-2.5, with the lower limit fixed by the chemical fog effect and the upper limit given by saturation. The observed intensity values are in general digitalized between 0 and 255.



Roentgen, 22 Dicembre 1895



Latent image detectors: Photographic film

The main advantages of the photographic film are:

- big dimensions;
- excellent spatial resolution;
- low cost;

while the disadvantages are:

- off-line read-out system, which needs the user's intervention to change and develop the films;
- low DQE value;
- limited dynamic range.

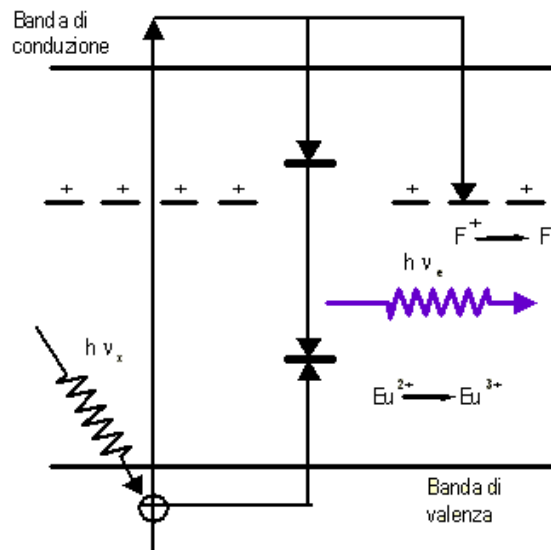


Roentgen, 22 Dicembre 1895

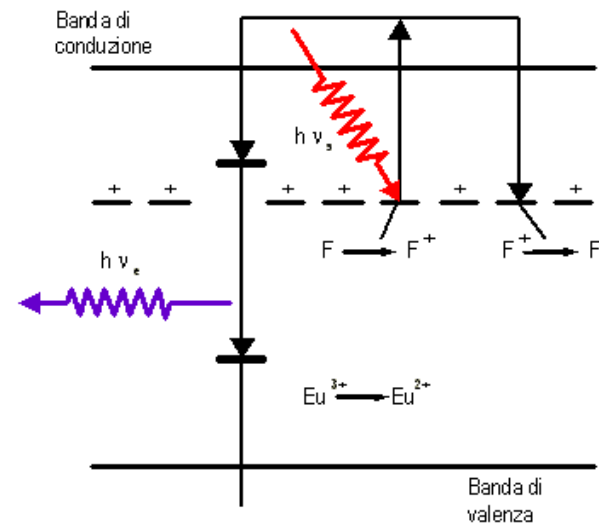


Latent image detectors: Imaging Plate

□ Imaging Plate - BaFBr:Eu²⁺



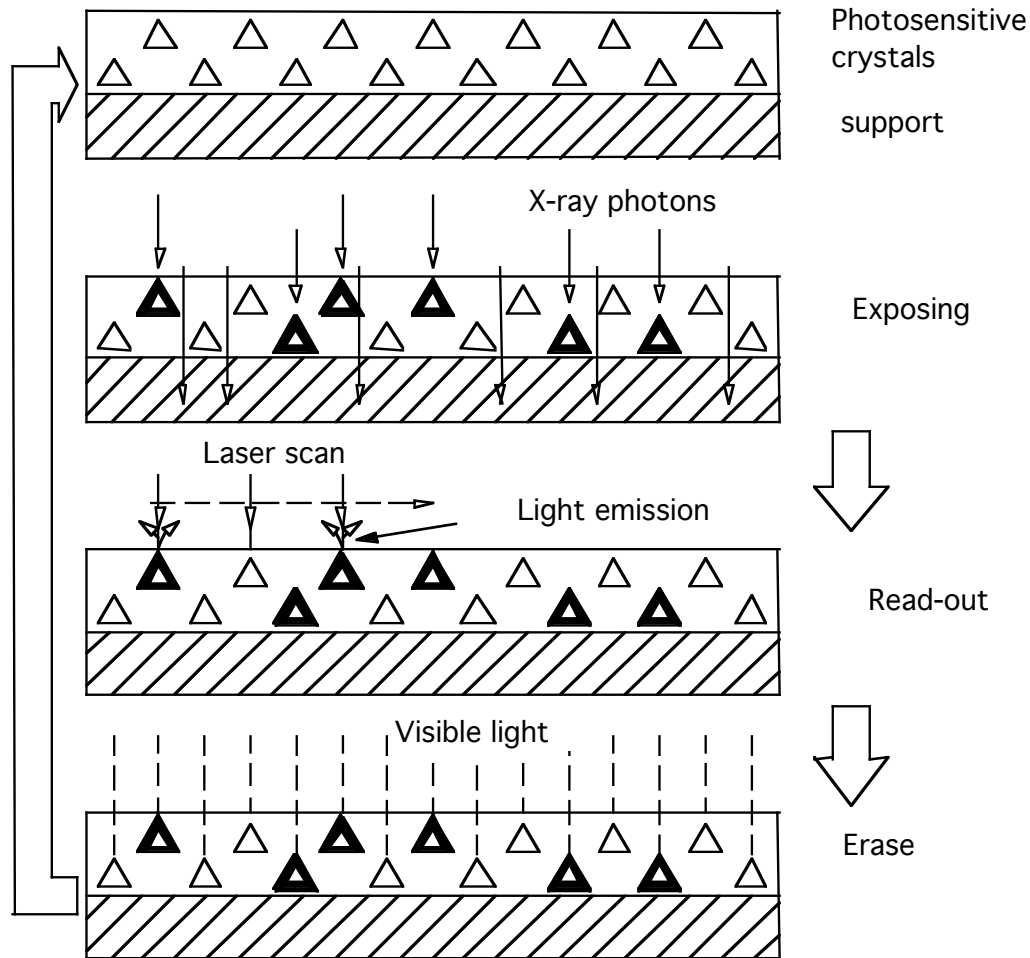
Esposizione ai raggi x



fotoluminescenza stimolata



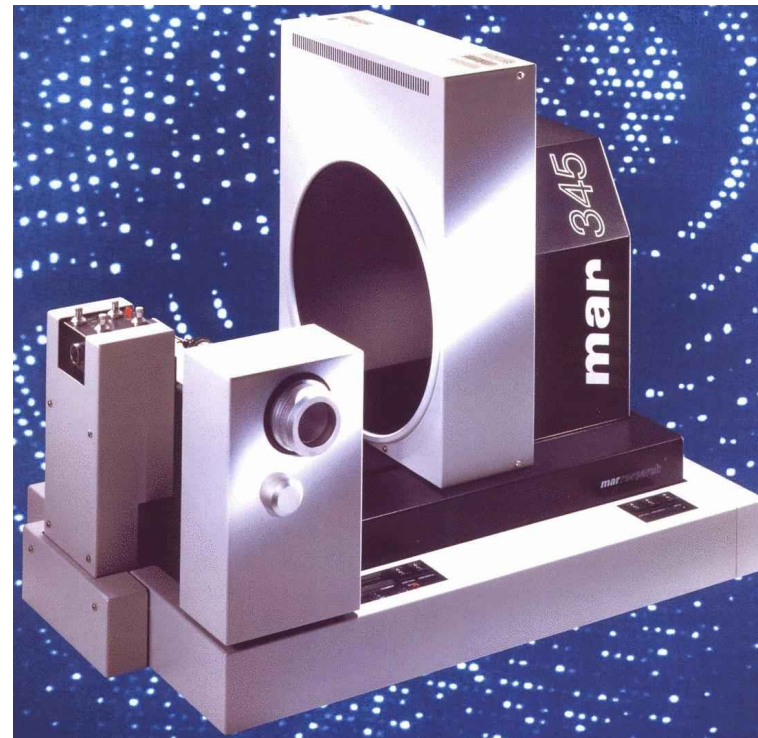
Exposure and Read-out Cycle of an Imaging plate



- • large lateral dimensions (up to 400 ´ 400 mm);
- • high efficiency in the 8-17 keV energy range;
- • PSF between 100 e 200 µm;
- • wide dynamic range
- The disadvantages are those connected with the fact that the IP is, like the photographic film, a latent image system, needing user's plate handling and/or poor duty cycle at the read-out.



Due esempi di Imaging plate

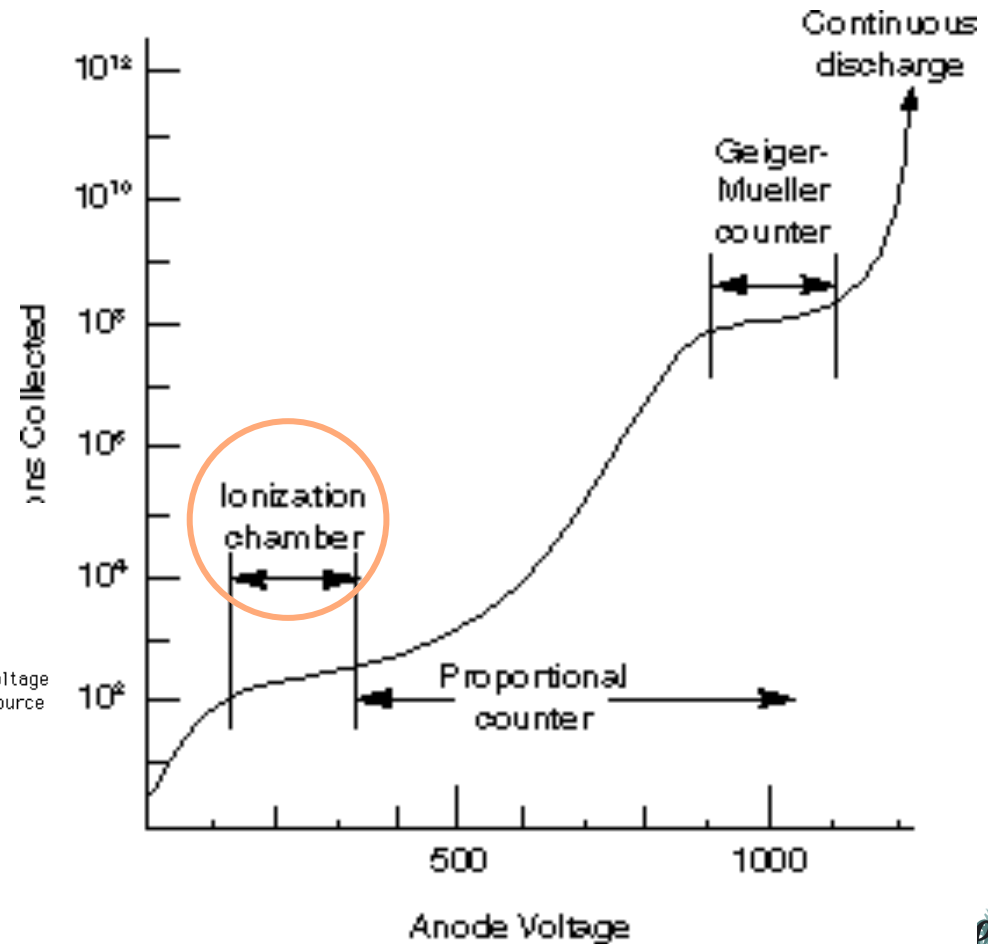
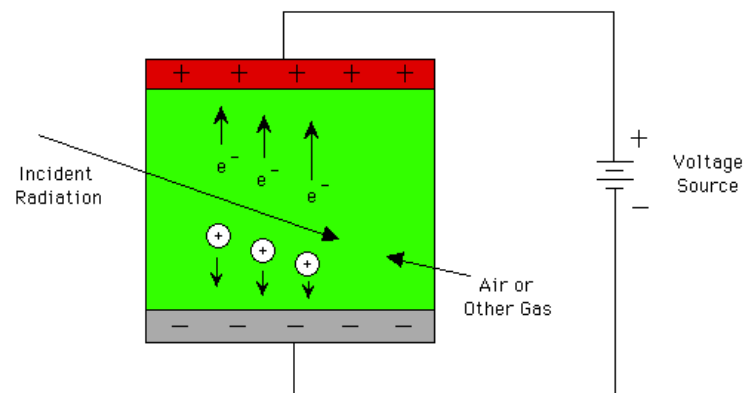


Gas detectors

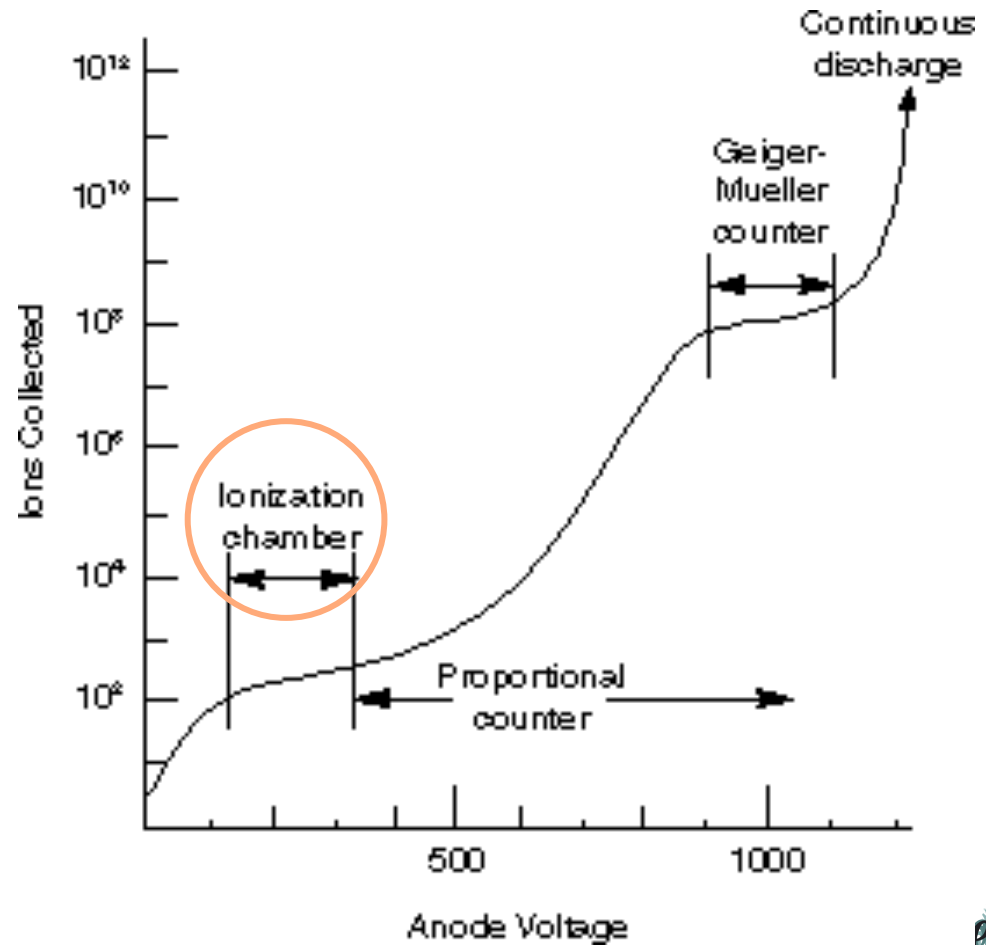
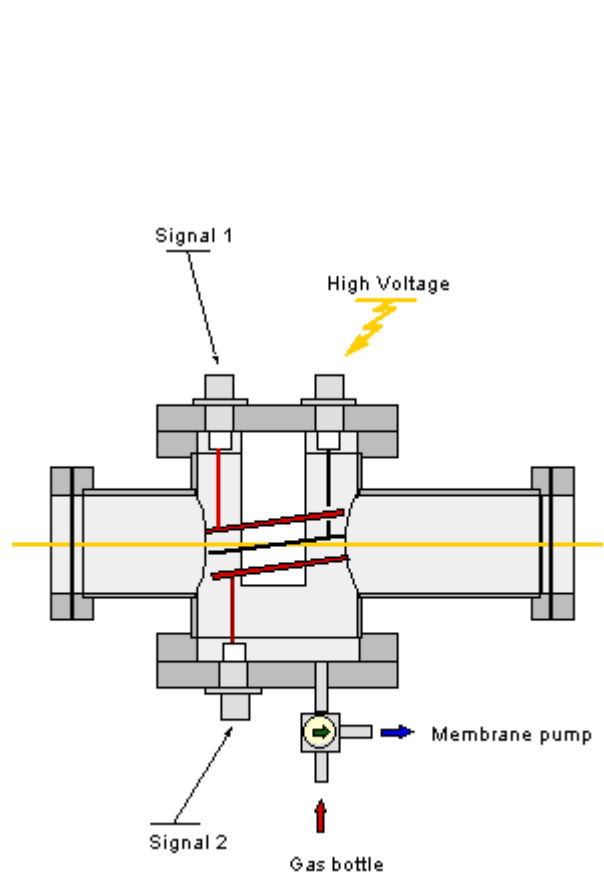
□ The absorption of the incoming X-ray photons in the gas molecules and the consequent creation of ion-electron pairs.

□ Ionisation chamber

□ $E_{event} = 26$ eV noble gas

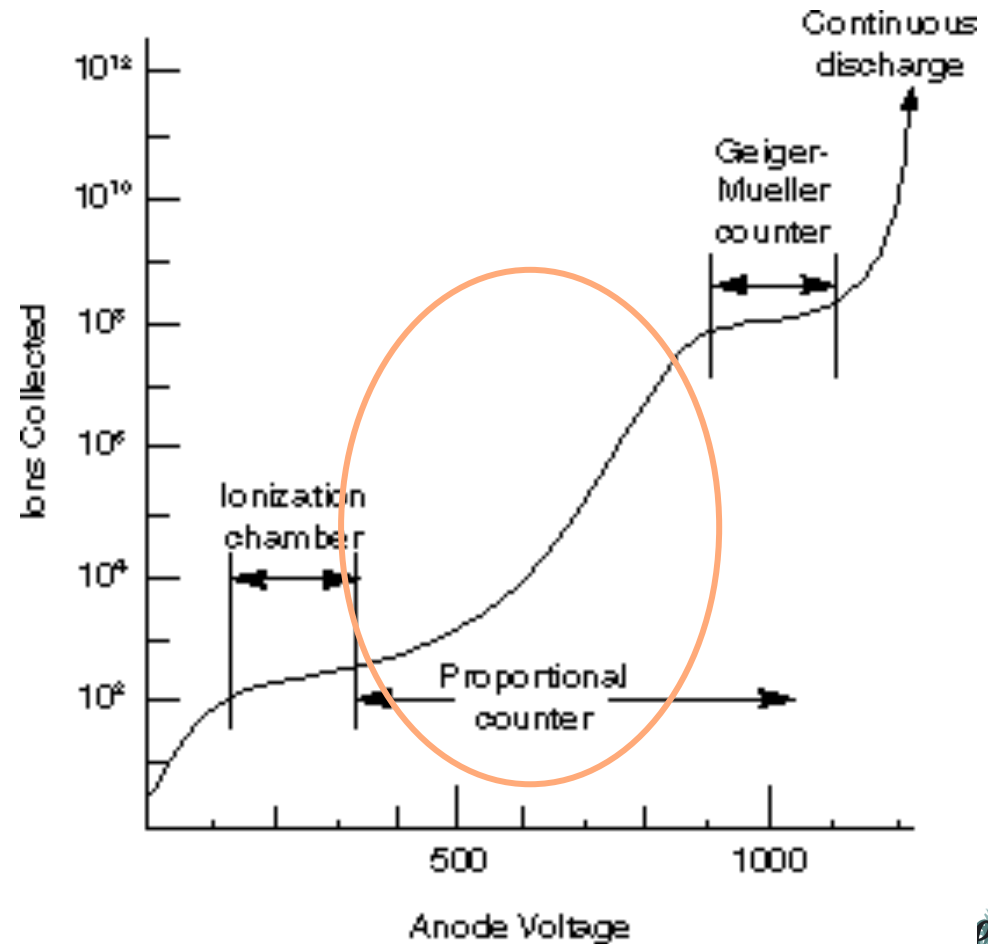


Ion Chamber as Beam Monitor



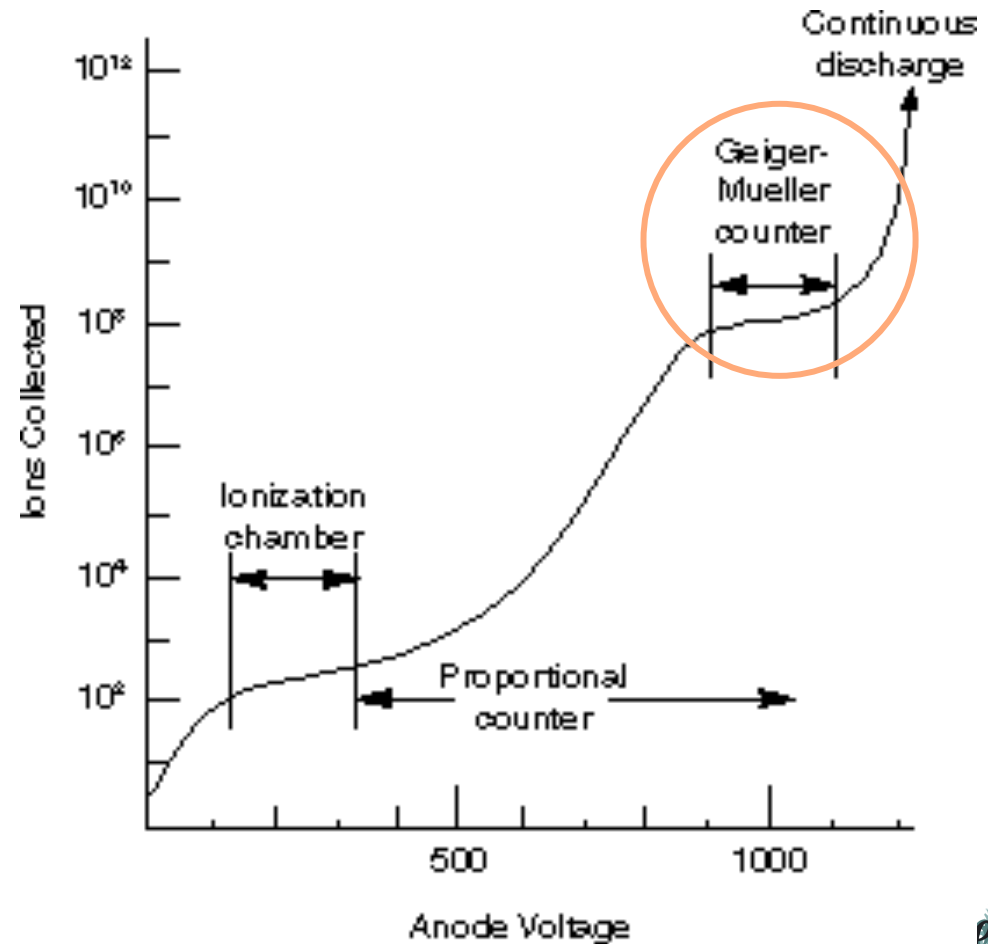
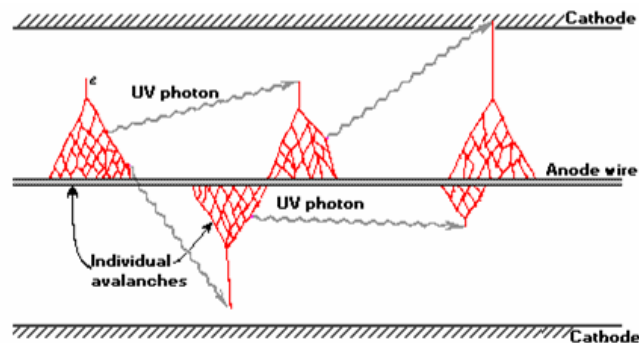
Proportional counters

Increasing the value of the potential applied between the electrodes, and providing a suitable mixture of gases, photoelectric absorption is followed by secondary ionisation avalanche, providing a charge gain up to 10^6 . The total charge collected from each photoelectric absorption event is proportional to the number of initial ion-electron pairs, and thus to the energy of the impinging photon.

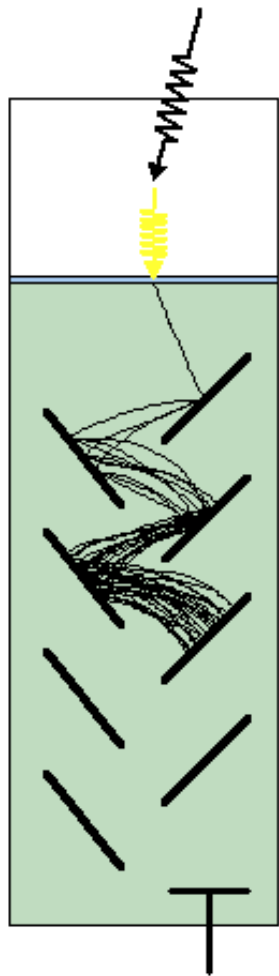


Geiger counter

Higher voltage accelerate the positive and negative charges, they gain more energy and collide with more atoms to release more electrons and positive ions; the process escalates into an avalanche which produces an easily detectable pulse of current. The gain is approx. 10^8



Scintillator Counters



One 5 keV photon
 ↓
 200 visible photons
 ↓
 30 photoelectrons
 ↓
 Gain around 10^6
 ↓
 Anode 3×10^7

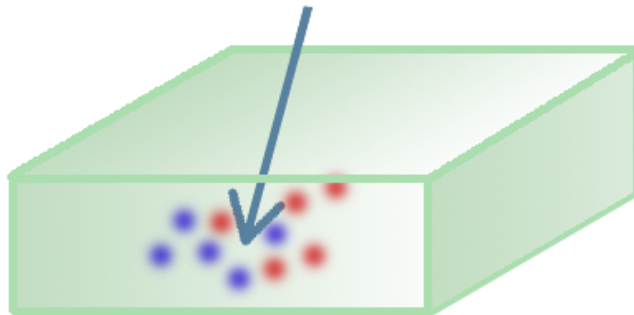
- pros
- High DQE up to 100 keV
 - Count rate up to 10^6

- cons
- Low energy resolution
(50% @ 8 keV)

| | NaI(Tl) | CsI(Na) | CsI(Tl) |
|--|---------|---------|---------|
| Good conversion efficiency (phot/keV) (% to NaI(Tl)) | 100 | 85 | 45 |
| Emitted light wavelength (nm) | 410 | 420 | 565 |
| Decay time (μ s) | 0.23 | 0.63 | 1.0 |
| Density (g/cm ³) | 3.67 | 4.51 | 4.51 |



Semiconductors



Electron-hole pairs are separated before recombination applying a potential difference; the amplitude of the signal is proportional to the energy of the photon

- E_{event} is much lower than for gases
 - 3.6eV per Si
 - 2.9 eV per Ge

» better energy resolution

Large Bandgap to minimise thermal noise

Narrow Bandgap to maximise statistics

Cooled devices



High Purity Ge:



Pros

Best energy resolution
(150 eV a 8 keV)

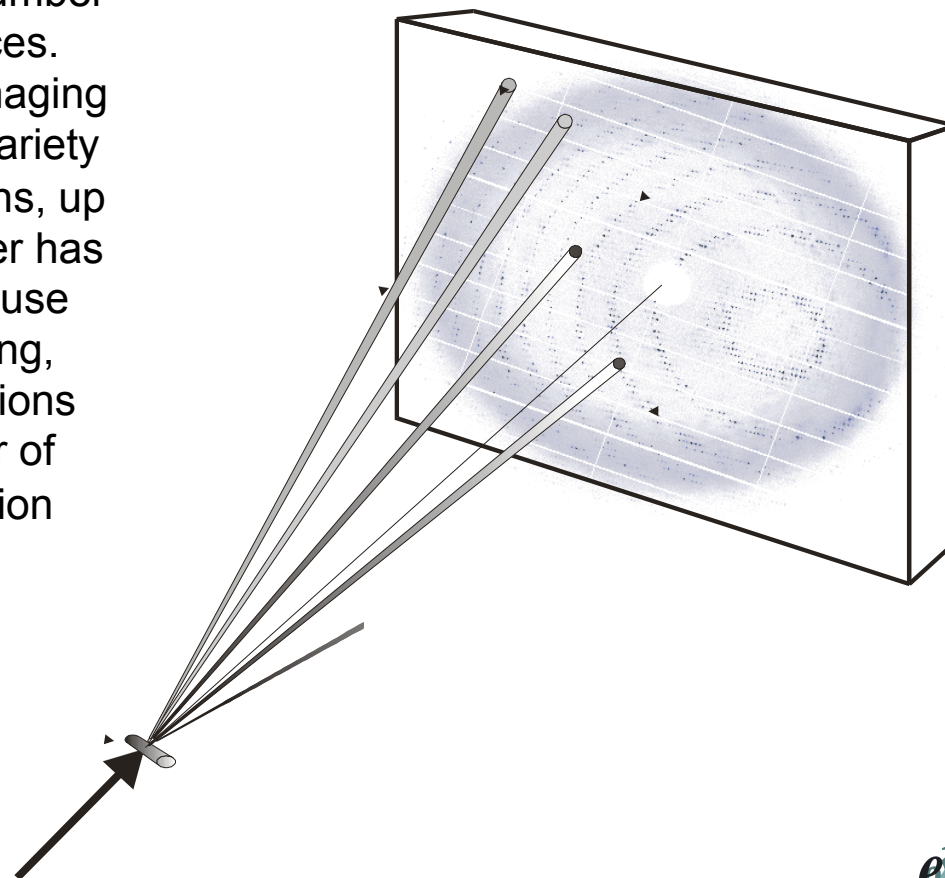
Cons

Bulky, heavy device
Cryostat needed
Low counting rate – 10^4 photons/s



Macromolecular crystallography / CCD

The strong investments of consumer's electronics made available a large number of CCD models, at reasonable prices. Originally designed for visible light imaging applications, these are offered in a variety of pixel sizes and of lateral dimensions, up to several centimetres. This wide offer has stimulated the research in order to use these devices also for X-ray imaging, resulting in a broad spectra of solutions devised and an increasing number of commercial available X-ray detection system.

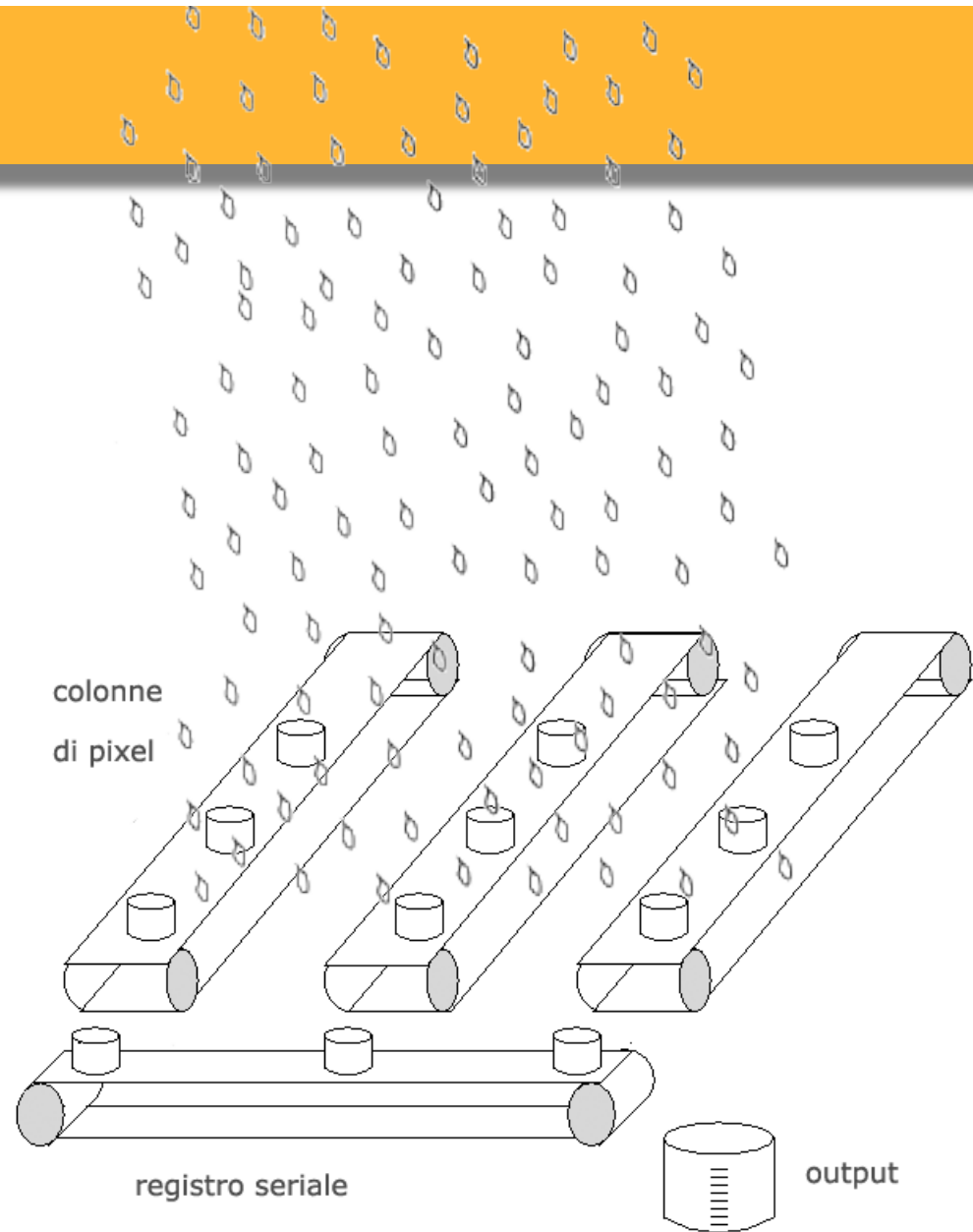


CCD according to J. Kristian

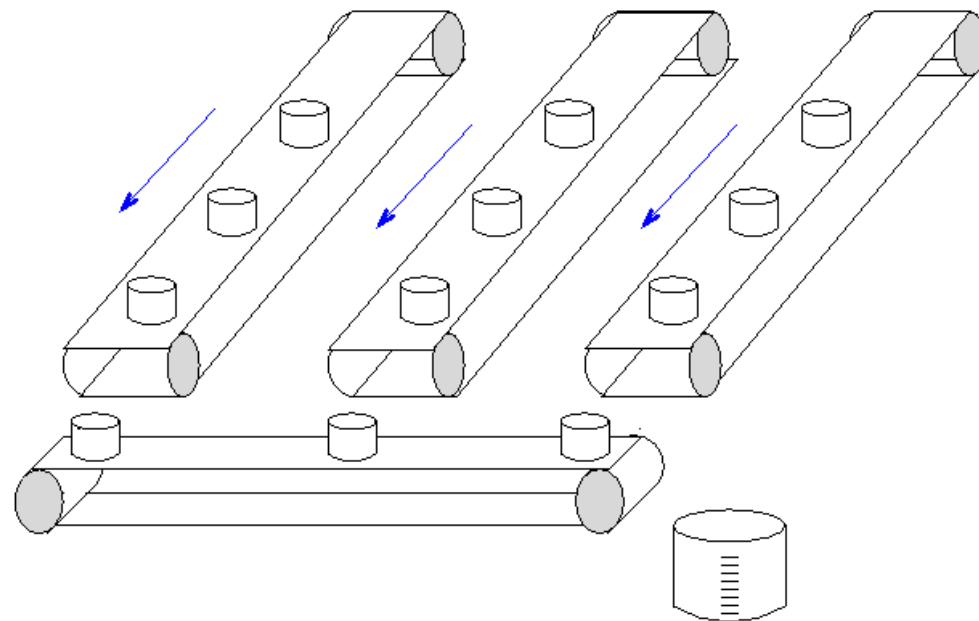
- > 1Megapixel
- pixel $\sim 20 \times 20 \mu\text{m}^2$
- Active area $> 20 \times 20 \text{mm}^2$
- DQE $\sim 0.2 - 0.3$
- Pixel to pixel charge transfer efficiency: 0.999997

Pros:

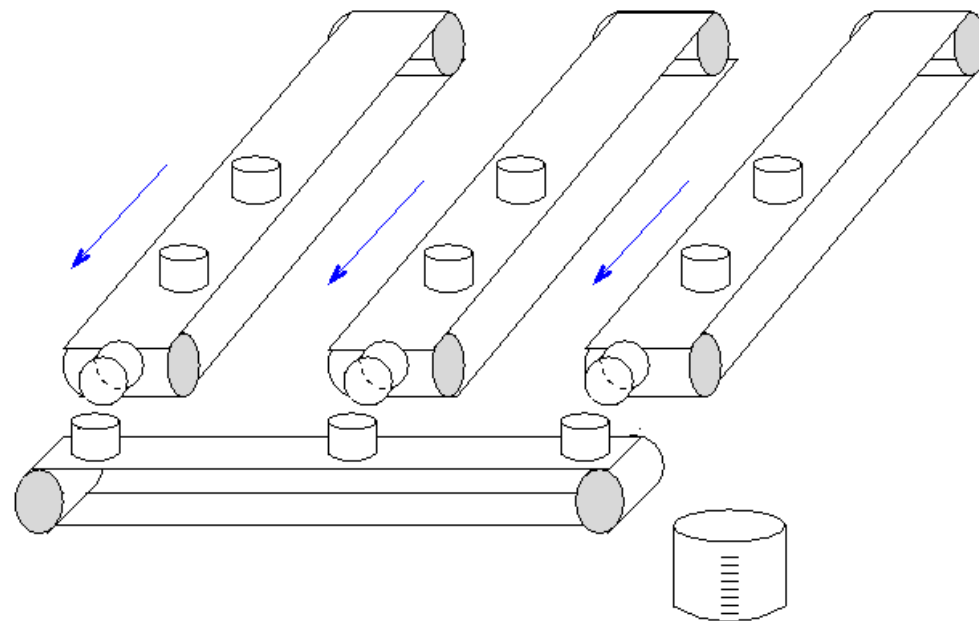
- stability
- Low consumption
- Linearity
- Compact
- Mass production



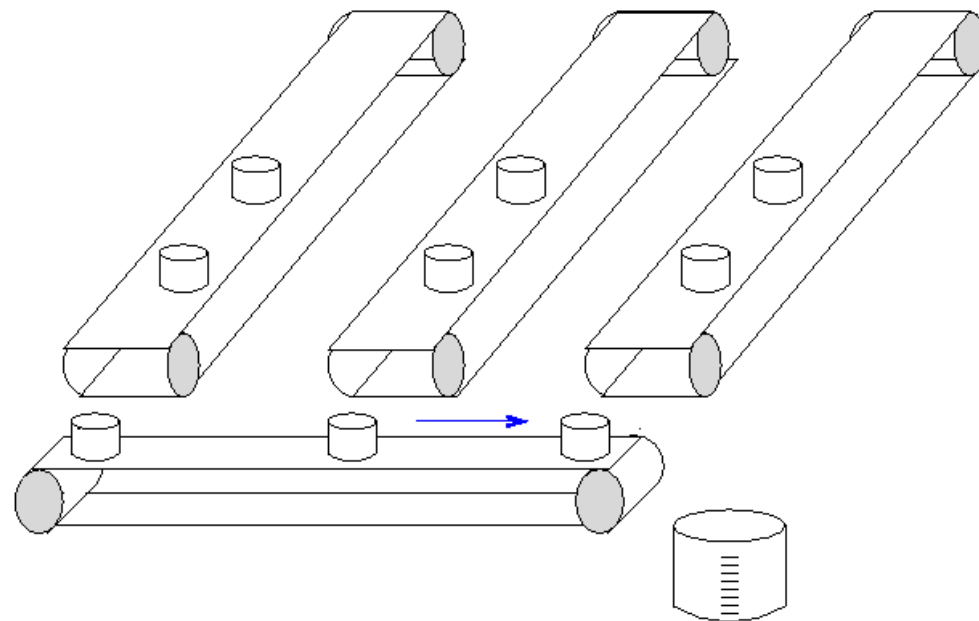
CCD according to J. Kristian

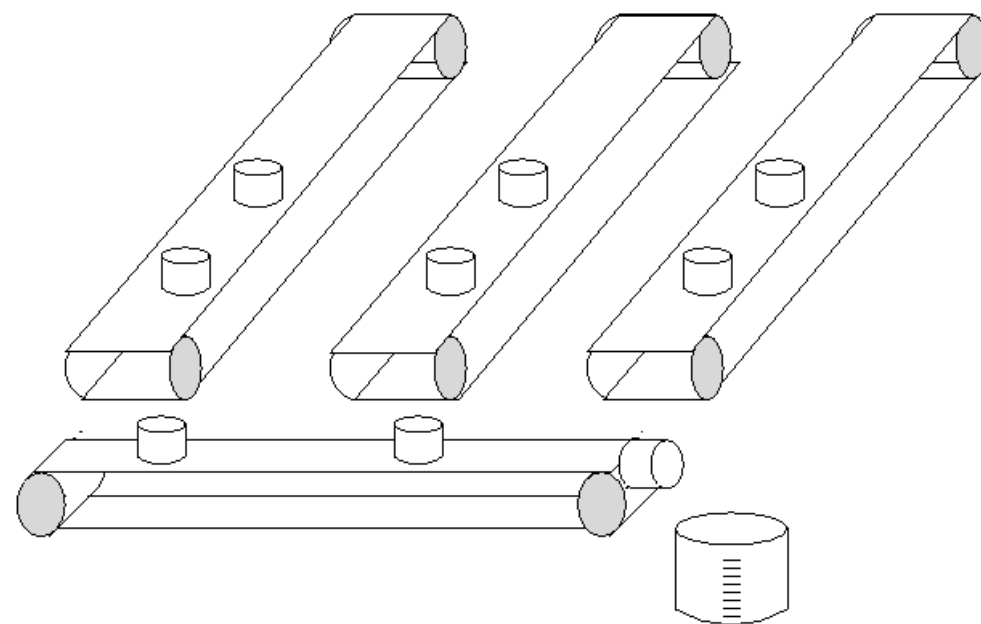


CCD according to J. Kristian

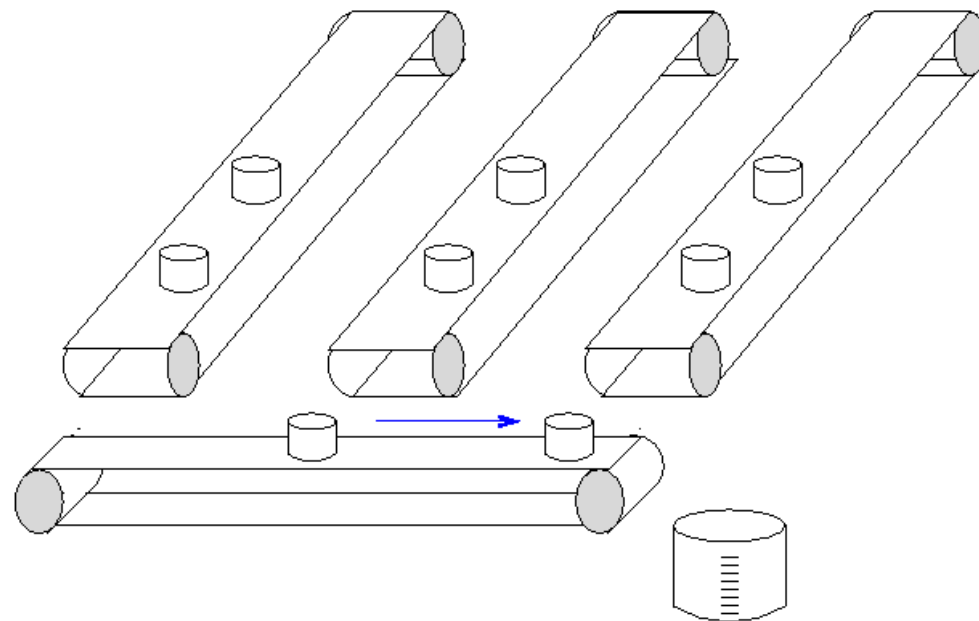


CCD according to J. Kristian

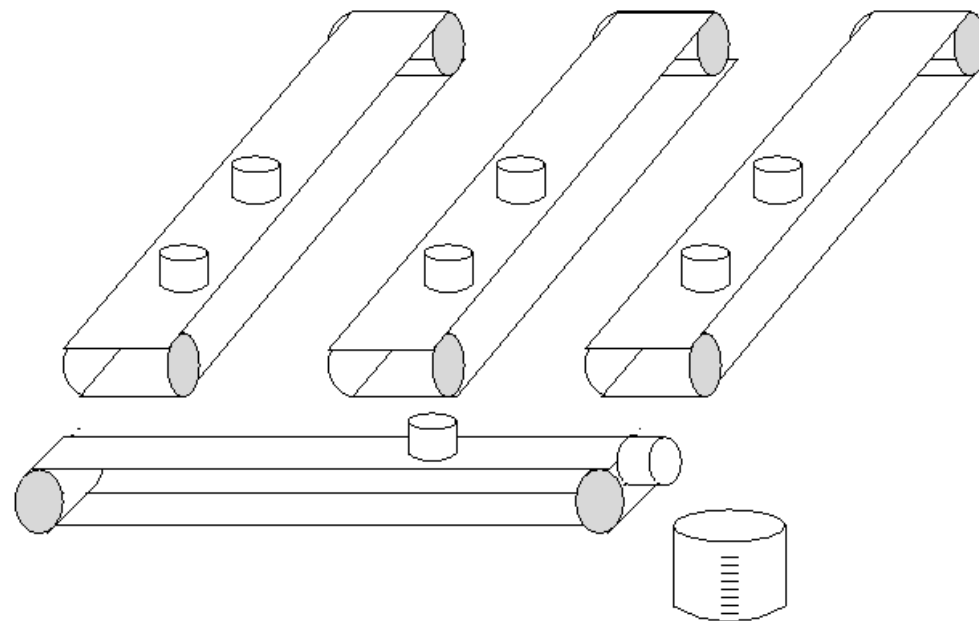




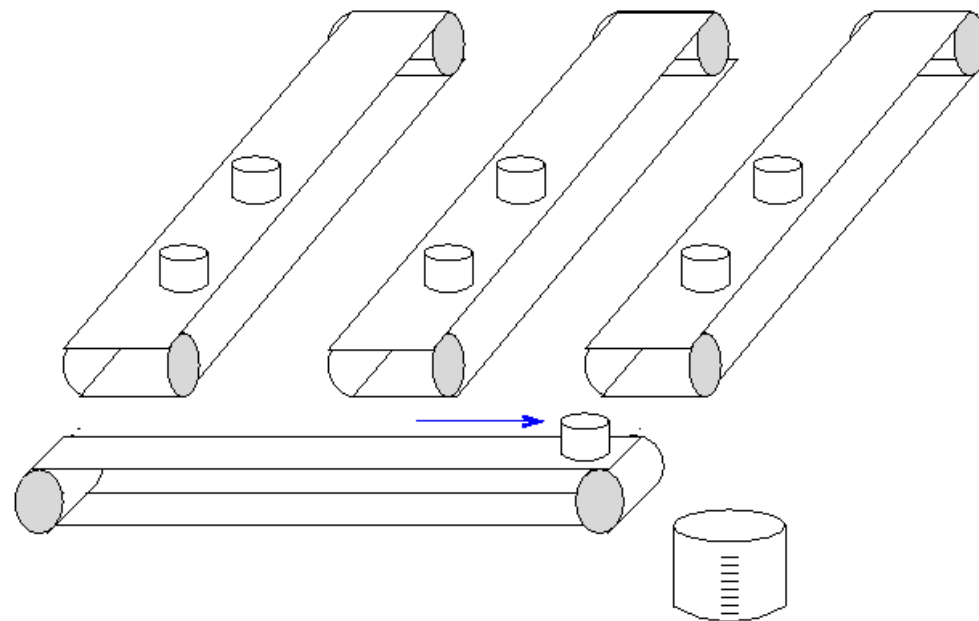
CCD according to J. Kristian



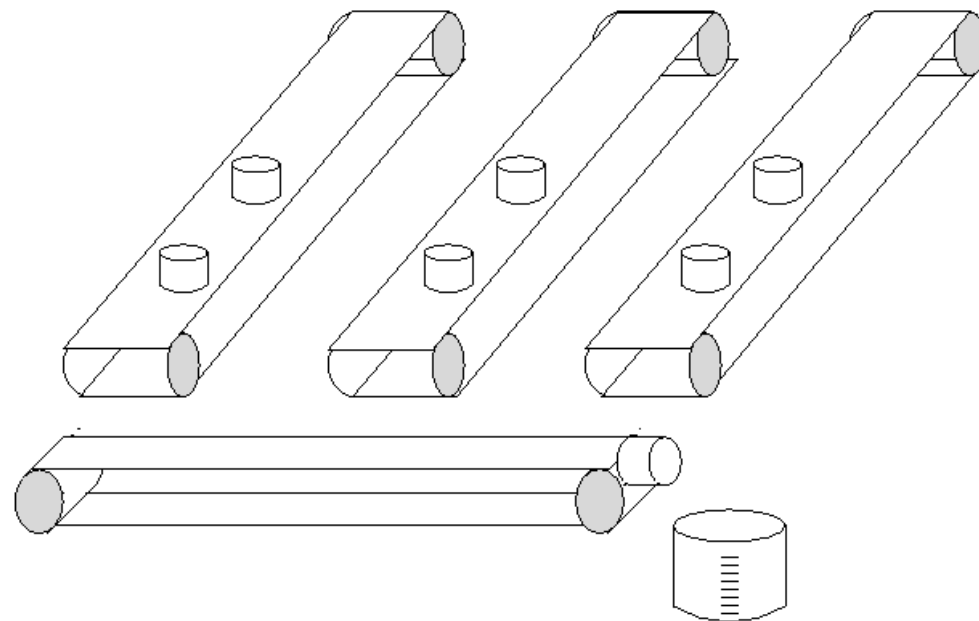
CCD according to J. Kristian



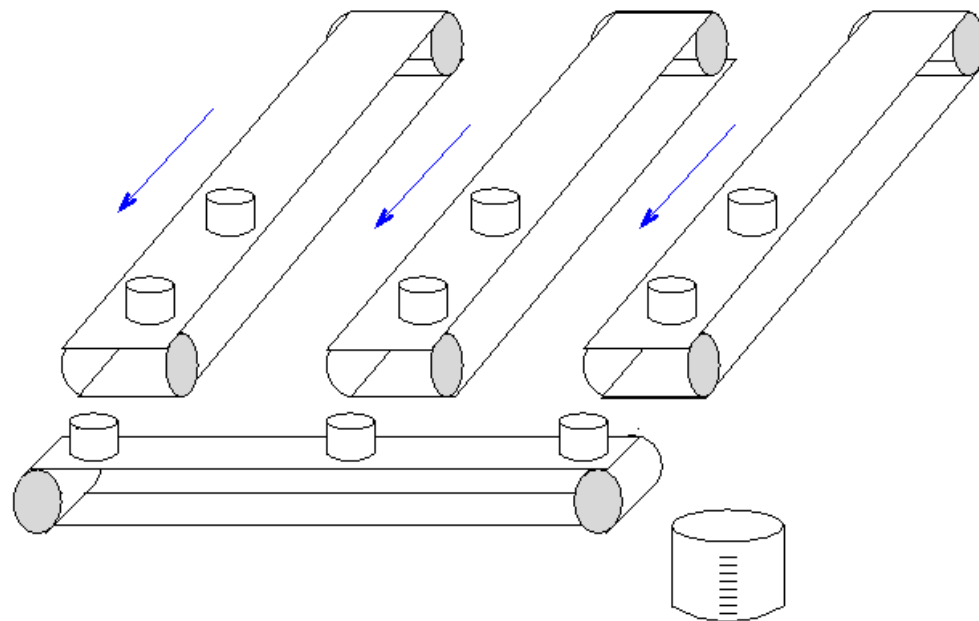
CCD according to J. Kristian



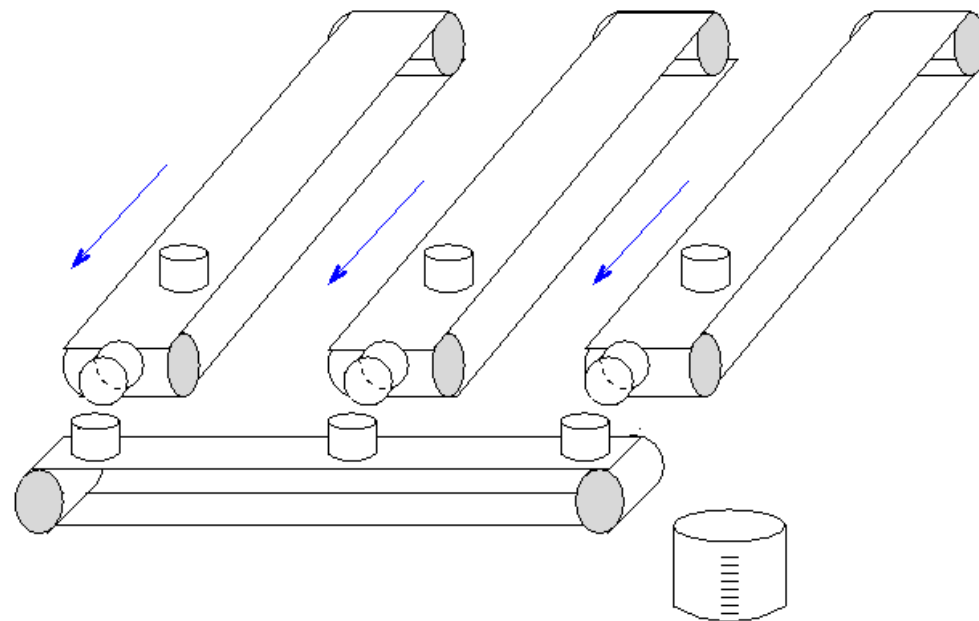
CCD according to J. Kristian



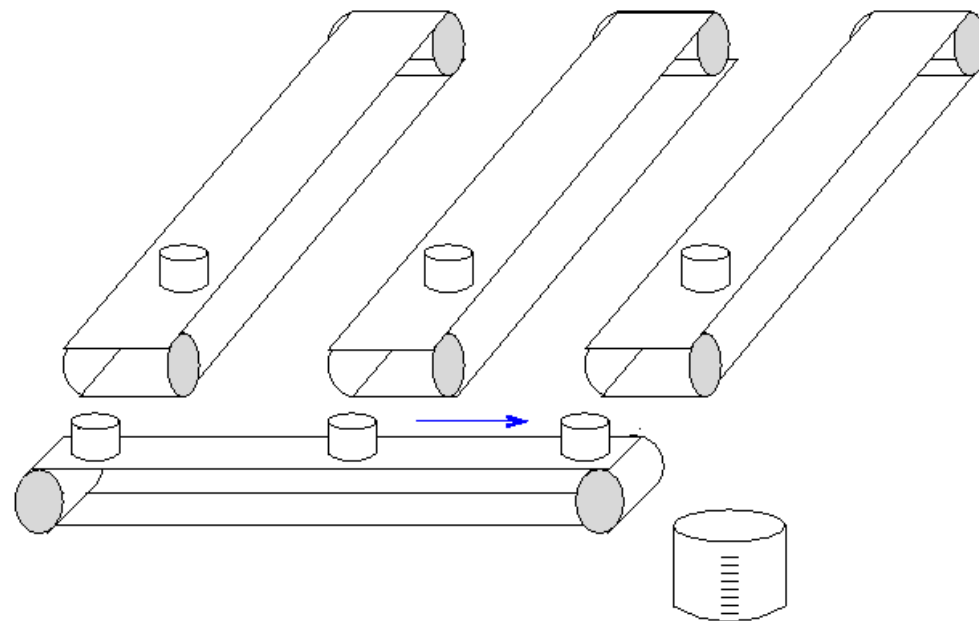
CCD according to J. Kristian



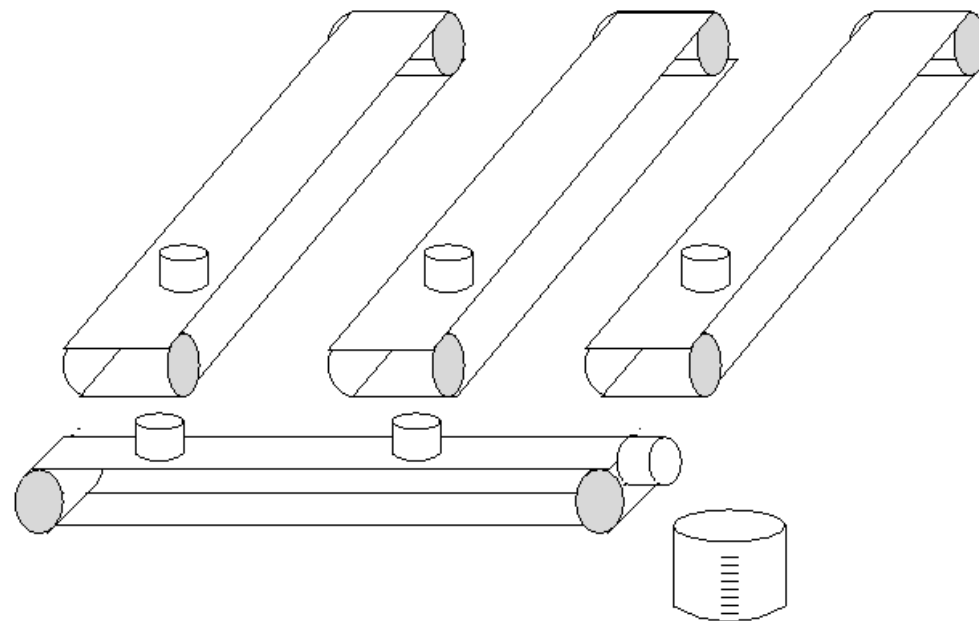
CCD according to J. Kristian



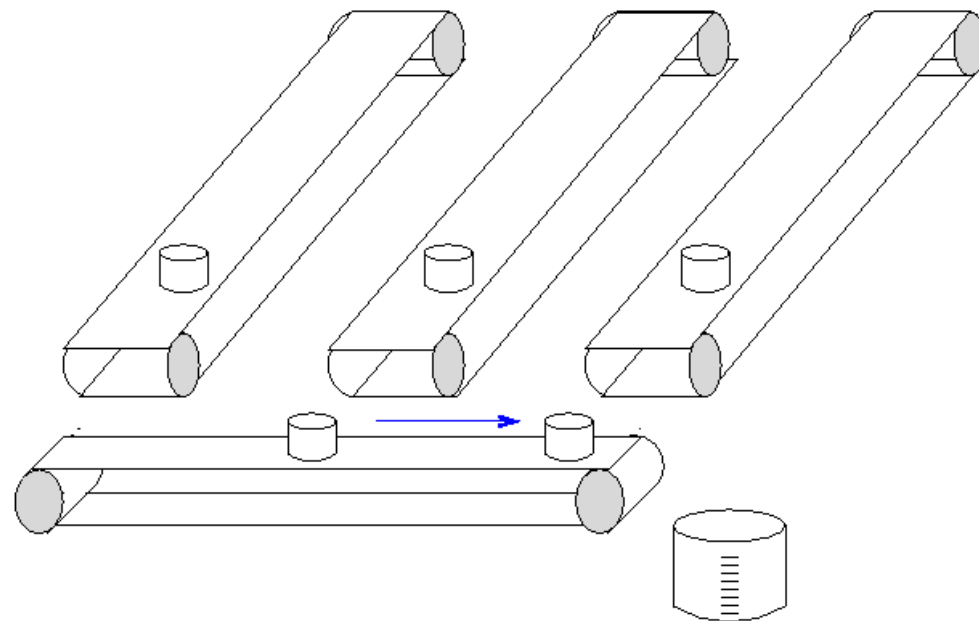
CCD according to J. Kristian



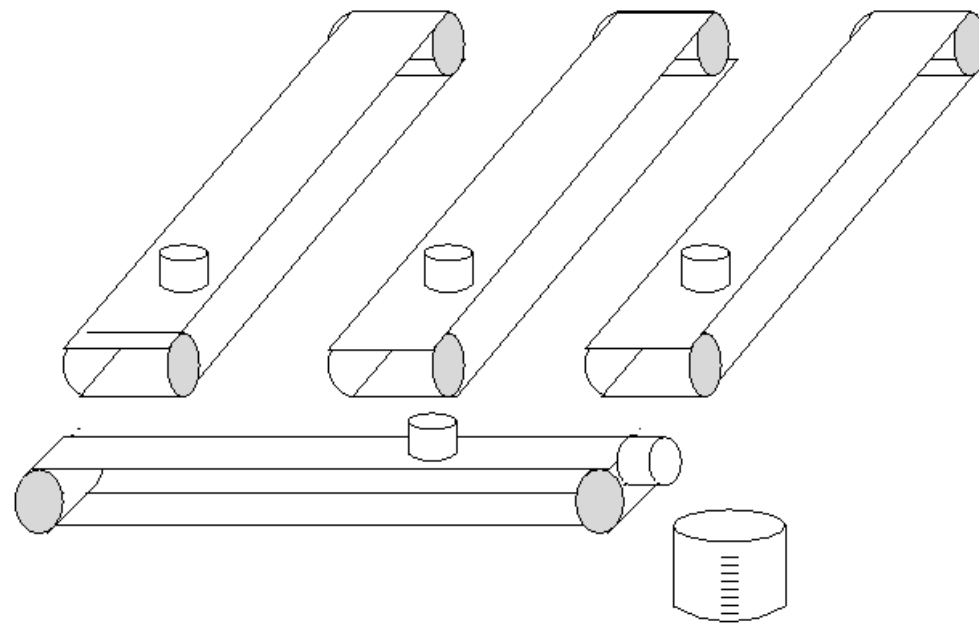
CCD according to J. Kristian



CCD according to J. Kristian



CCD according to J. Kristian



CCD according to J. Kristian

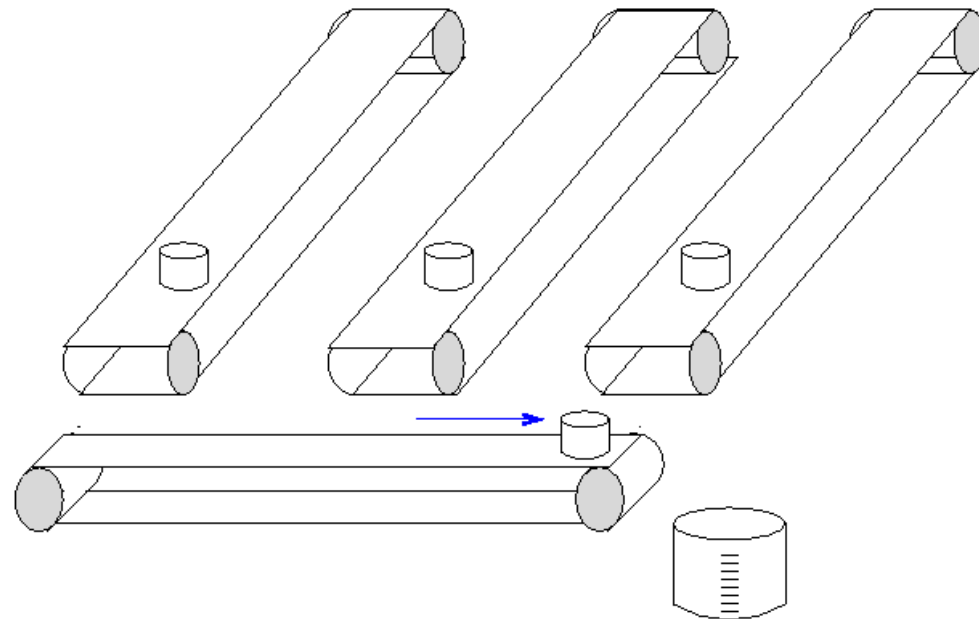
- > 1Megapixel
- pixel $\sim 20 \times 20 \mu\text{m}^2$
- Active area $> 20 \times 20 \text{mm}^2$
- DQE $\sim 0.2 - 0.3$
- Pixel to pixel charge transfer efficiency: 0.999997

Pros:

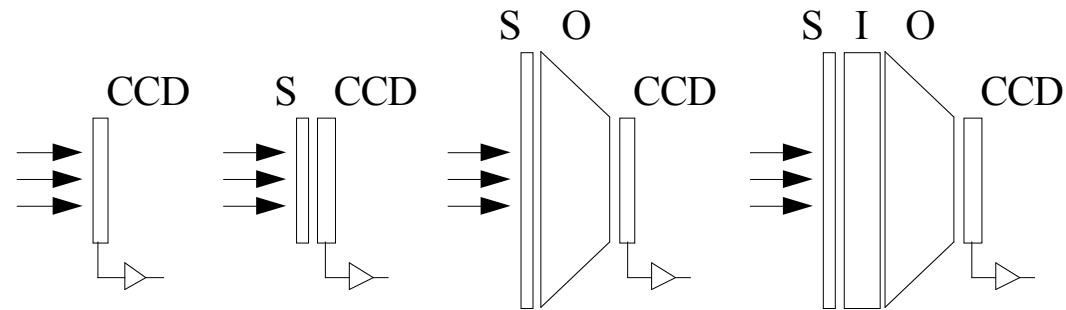
- stability
- Low consumption
- Linearity
- Compact
- Mass production

Cons:

- Too small for many applications
- Sequential read-out (slow)
- Prone to radiation damage



CCD as x ray detector



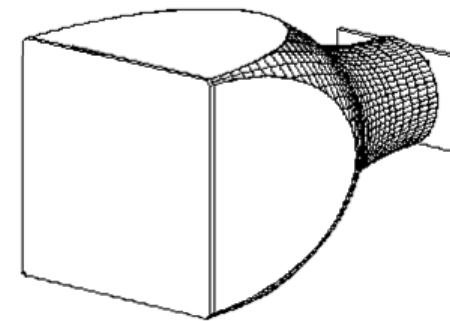
- Direct illumination
- Scintillatore or phosphor screen (S) in direct contact with the sensor
- Larger screen optically coupled to the CCD
- Image intensifier between the phosphor screen and the optical coupling



Screen + optical fiber

- Favorable form factor
- lighter
- Mechanically stable
- Efficient light transmission:

| demagnification | transmission |
|-----------------|--------------|
| 2:1 | 20% |
| 3:1 | 10% |



Cons

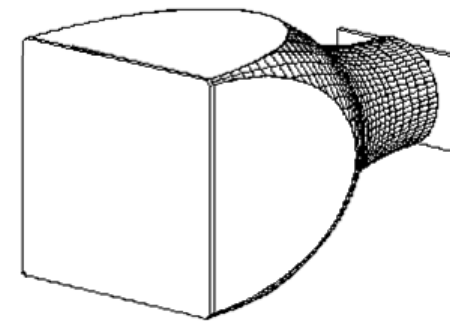
- Distorsions
- Extremely small depth-of-field
- Interference fringes at interface



Screen + optical fiber

$\text{Gd}_2\text{O}_2\text{S:Tb}$

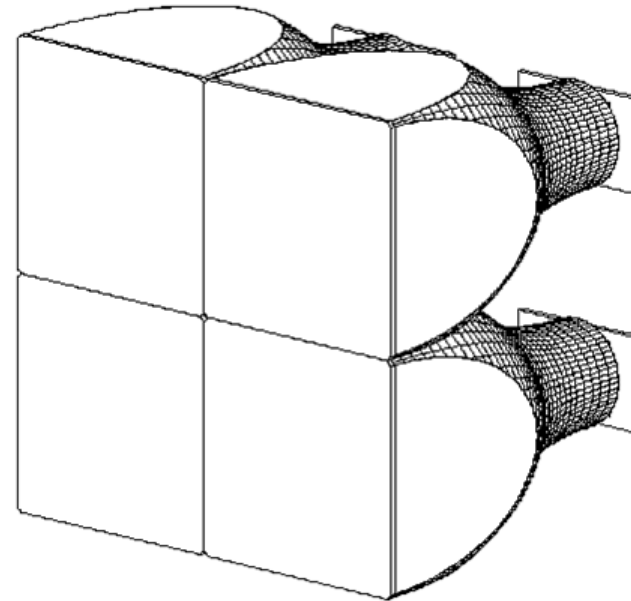
- High absorption efficiency
- density $\sim 8 \text{ gm/cm}^3$
- $\text{Gd}_2\text{O}_2\text{S:Tb}$ thin films ($10 \mu\text{m}$) can be deposited directly on the optical fiber terminations, ensuring 97% absorption efficiency at 8keV
- Decay time $\sim 3 \text{ ms}$



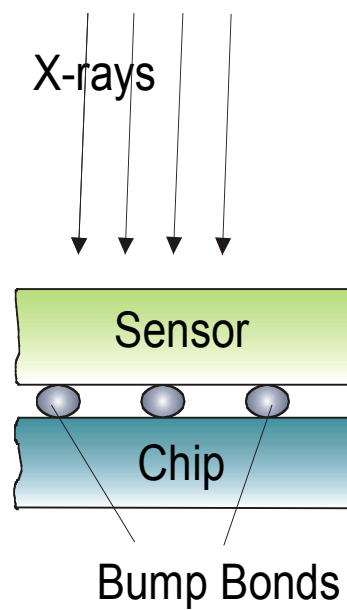
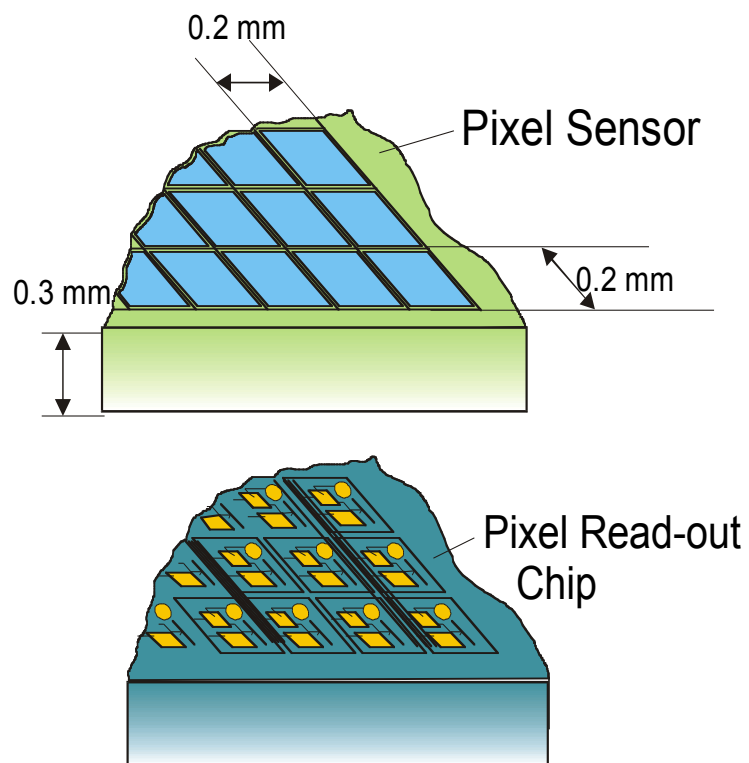
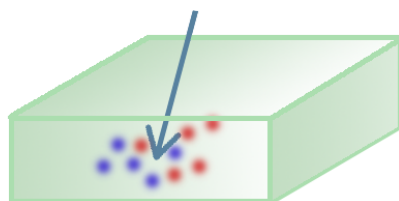
Screen + optical fiber

$\text{Gd}_2\text{O}_2\text{S:Tb}$

- High absorption efficiency
- density $\sim 8 \text{ gm/cm}^3$
- $\text{Gd}_2\text{O}_2\text{S:Tb}$ thin films ($10 \mu\text{m}$) can be deposited directly on the optical fiber terminations, ensuring 97% absorption efficiency at 8keV
- Decay time $\sim 3 \text{ ms}$
- Can be tiled to get larger area



Pixel detector



Pilatus (SLS)

□PIXEL:

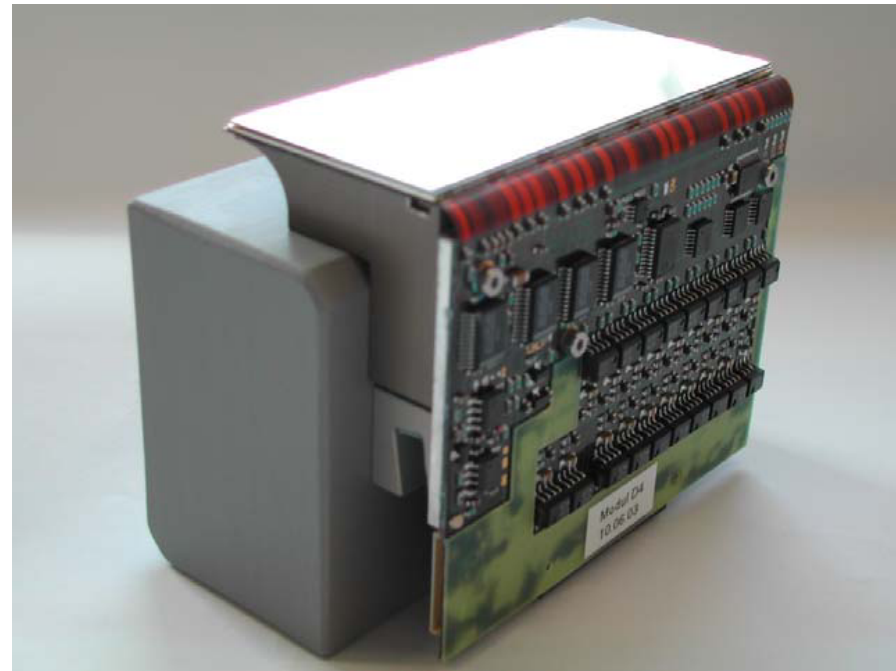
- $217 \times 217 \mu\text{m}^2$
- 15-bit counter
- $>10^5$ fotoni

□CHIP:

- 44×78 pixels, $10 \times 17.5 \text{ mm}^2$
- Read out @ 10 MHz

□MODULO:

- $80 \times 35 \text{ mm}^2$, 55Kpixels
- 16 chip in parallel
- Controller board



Pilatus (SLS)

□BANK:

- 3 modules
- 1 controller per module

□DETECTOR:

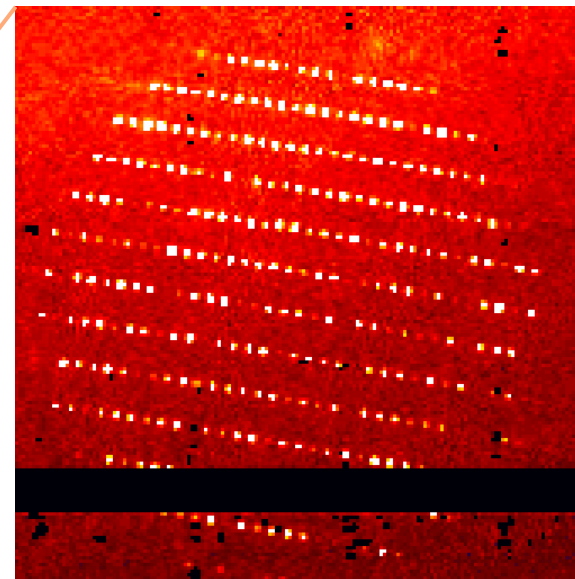
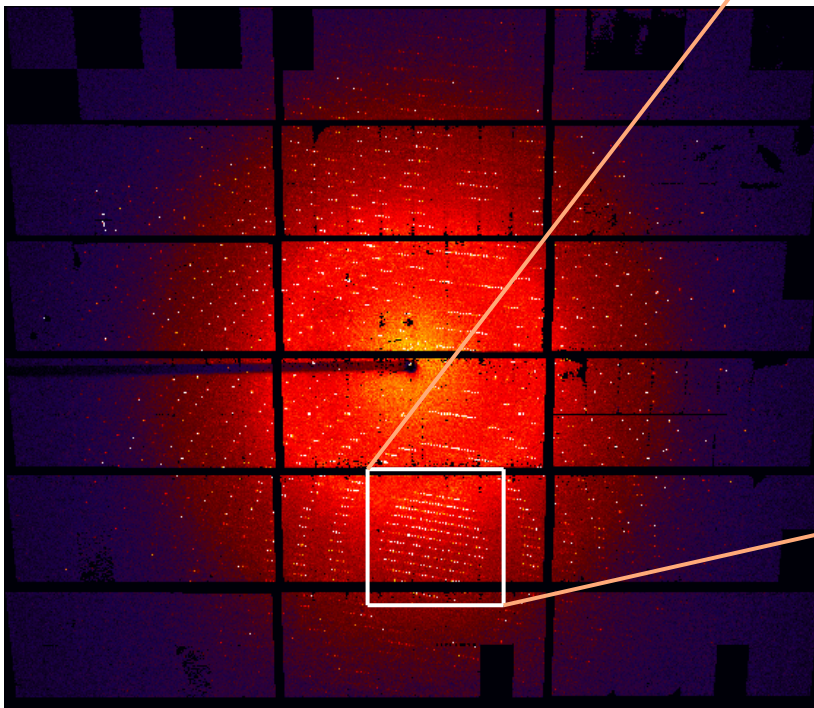
- 6 three-modules banks
- 1056 x 936 pixel
- Area: 21 x 24 cm²
- 288 chips->~300x10⁶ transistors
- 2 images/s
- Active Area: 85%

- Counting capabilities 10kHz/pixel
- 1Gb in 15' (180°)



Pilatus (SLS)

- Now: 12 five-modules banks
- 2000 images (16 GB) in ~3 min.



Phase Identification

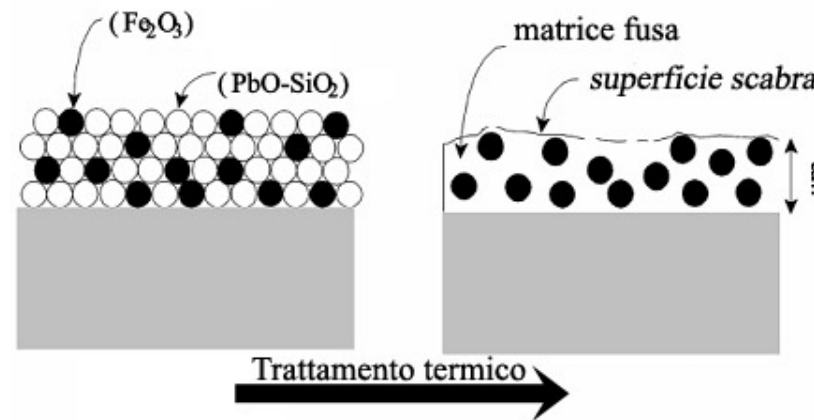


XIII-XVI sec.
End XV large stained glass windows

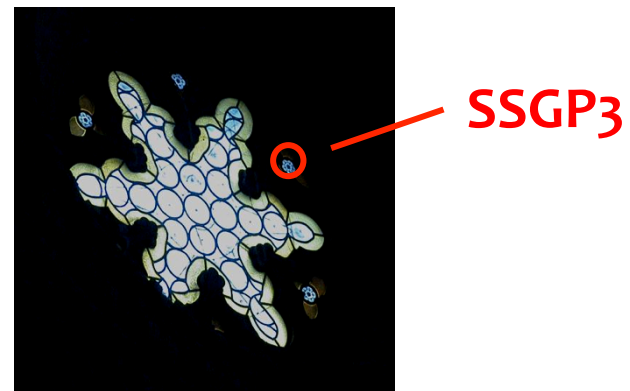
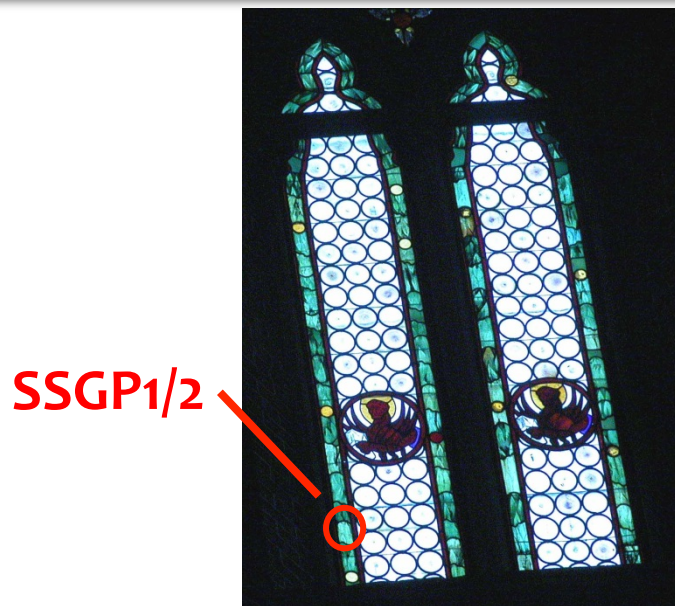


Grisaille technique

- Low melting glass (SiO_2 , PbO ,)
- Pigment (metal oxides)
- Paint medium (water, vinegar, oil)
- Firing to fuse the grisaille on the glass



Grisaille degradation



SSGP2



SSGP2



SSGP3



| Sample | Glass | Grisaille | Patina |
|--------|--------------|-----------|--------|
| SSGP1 | Green | Dark | Brown |
| SSGP2 | Green | Brown | White |
| SSGP3 | Light yellow | Blue | White |

SSGP2

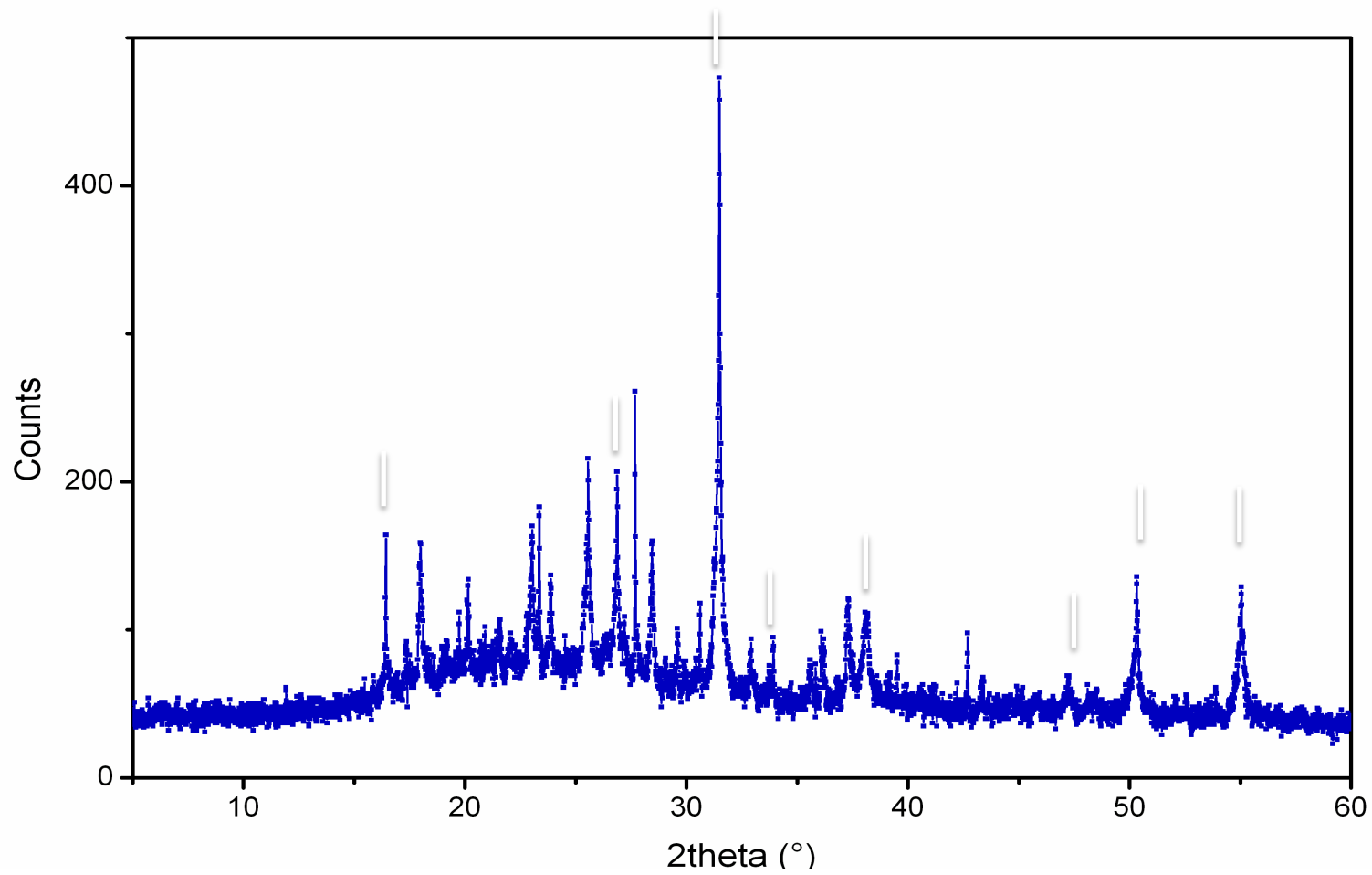


SSGP2



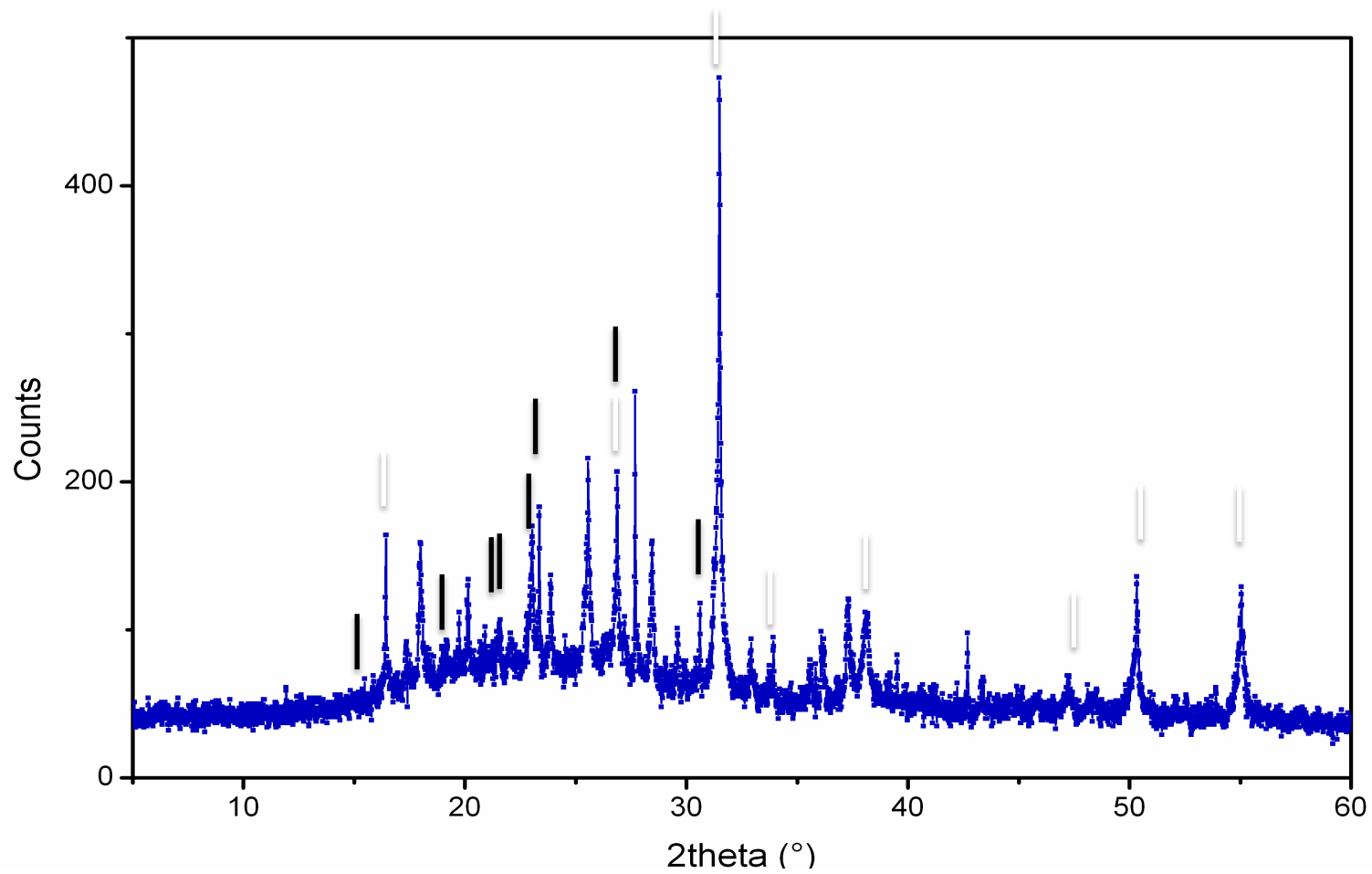
SSGP3





Spinel
 CoAl_2O_4
01-082-2422

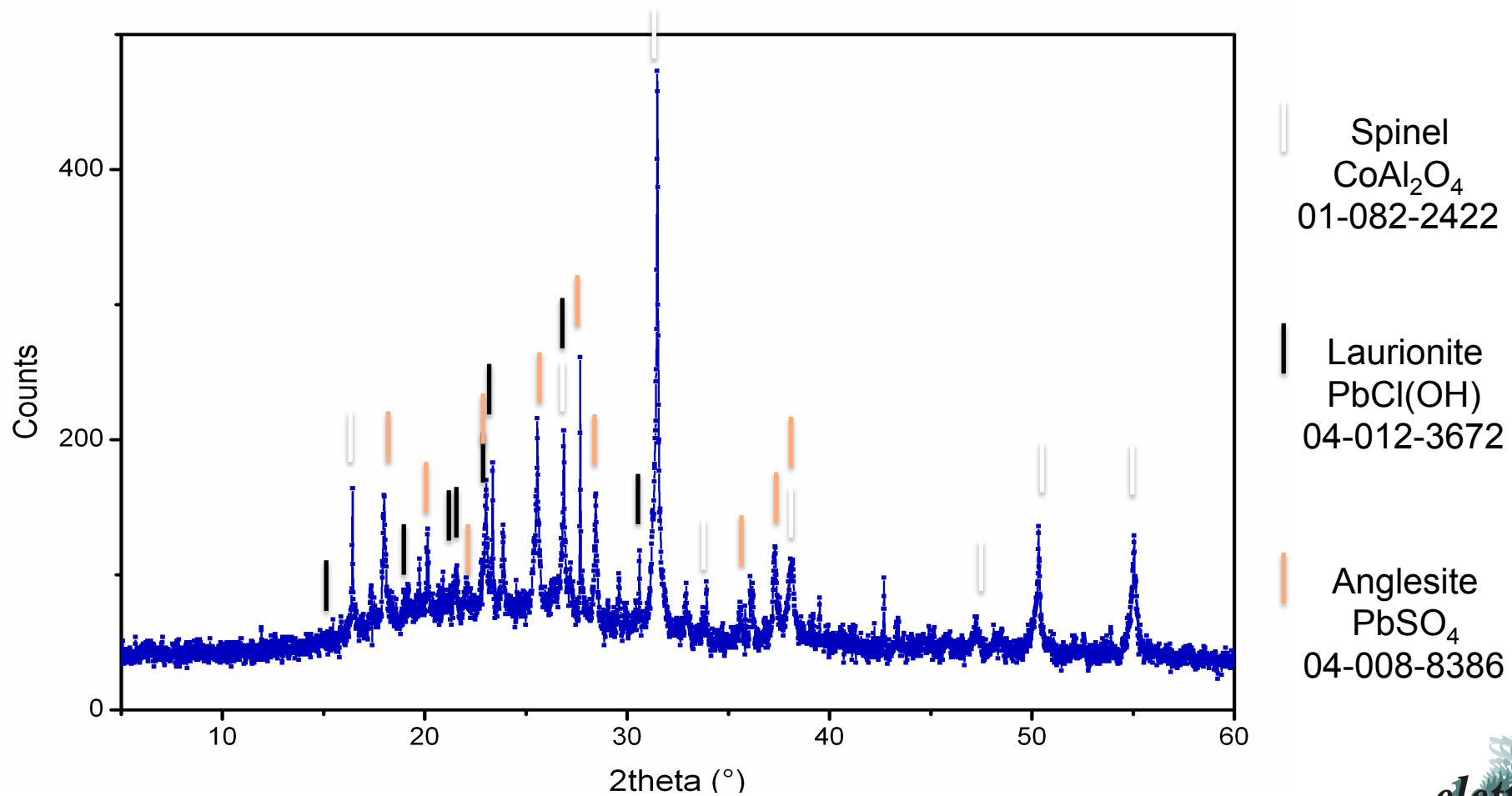




Spinel
CoAl₂O₄
01-082-2422

Laurionite
PbCl(OH)
04-012-3672

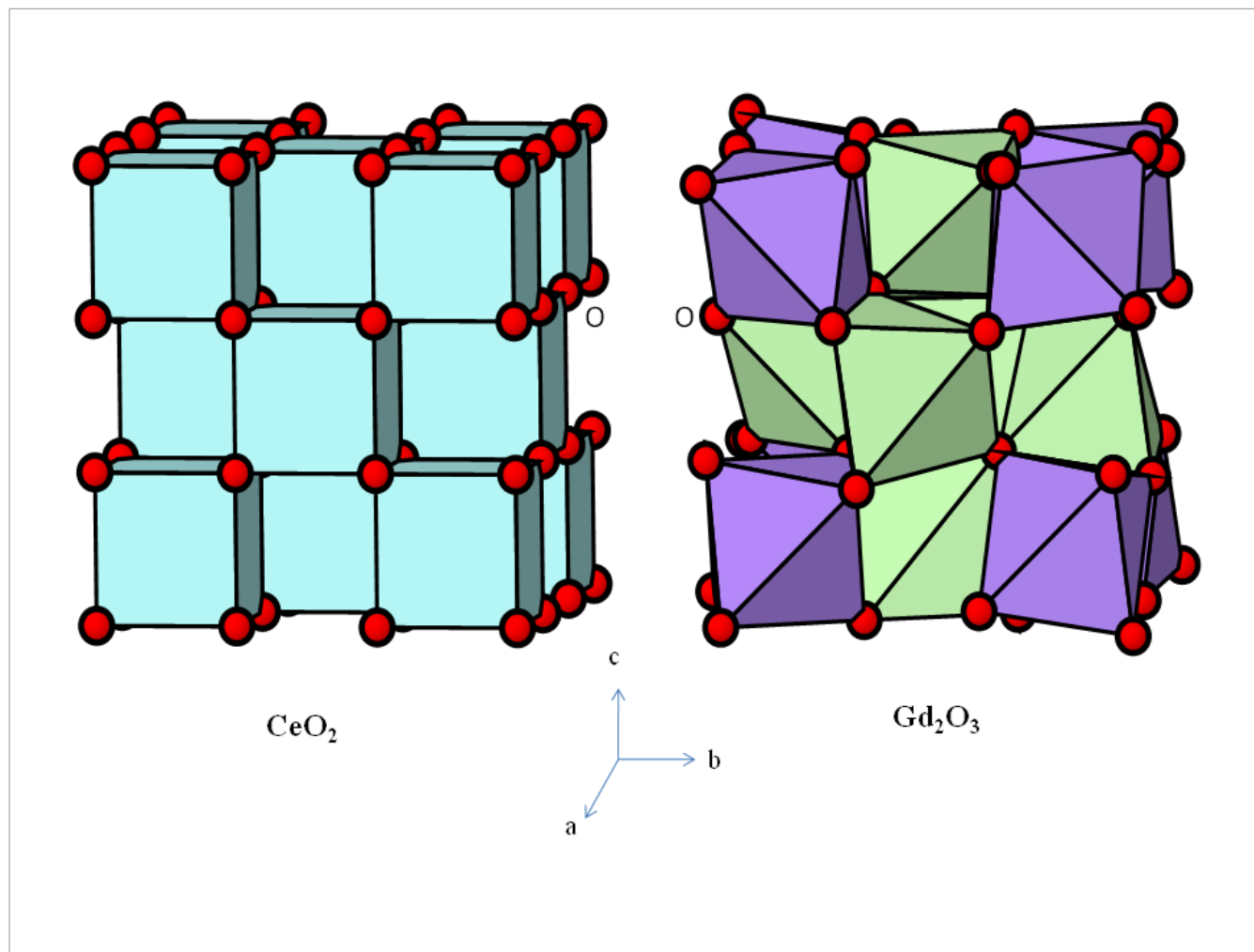


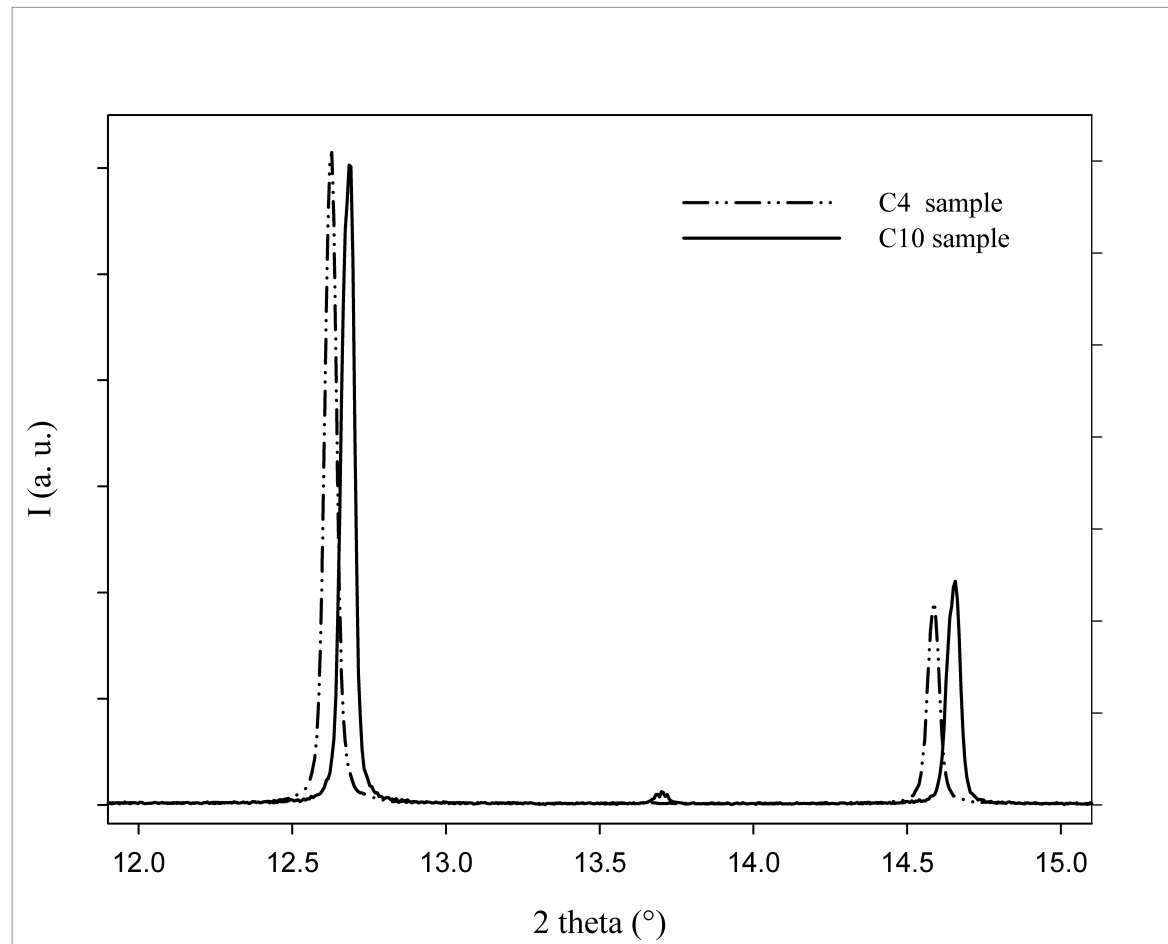


- $\text{Pb}_2\text{Sb}_2\text{O}_7$: original pigment
- SO_4^{2-} , S^{2-} , CO_3^{2-} : alteration product seawater-aerosol , acid rain
- $\text{FeO}(\text{OH})$; $\text{FeSO}_4(\text{OH})(\text{H}_2\text{O})_2$: alteration product of original pigments
- CO_3^{2-} , PO_3^{3-} : biological origin
- CoAl_2O_4 : intervention at later date?

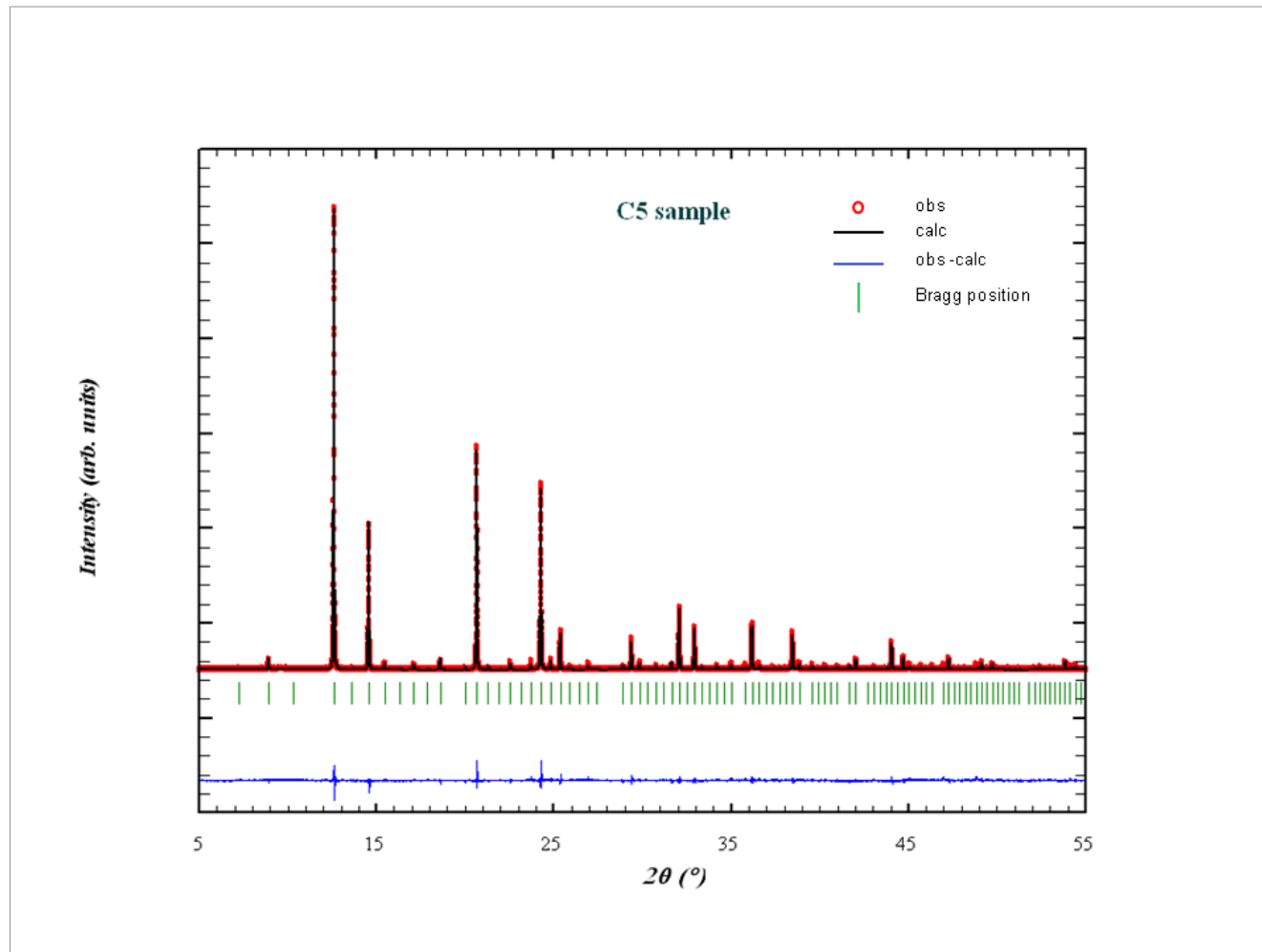


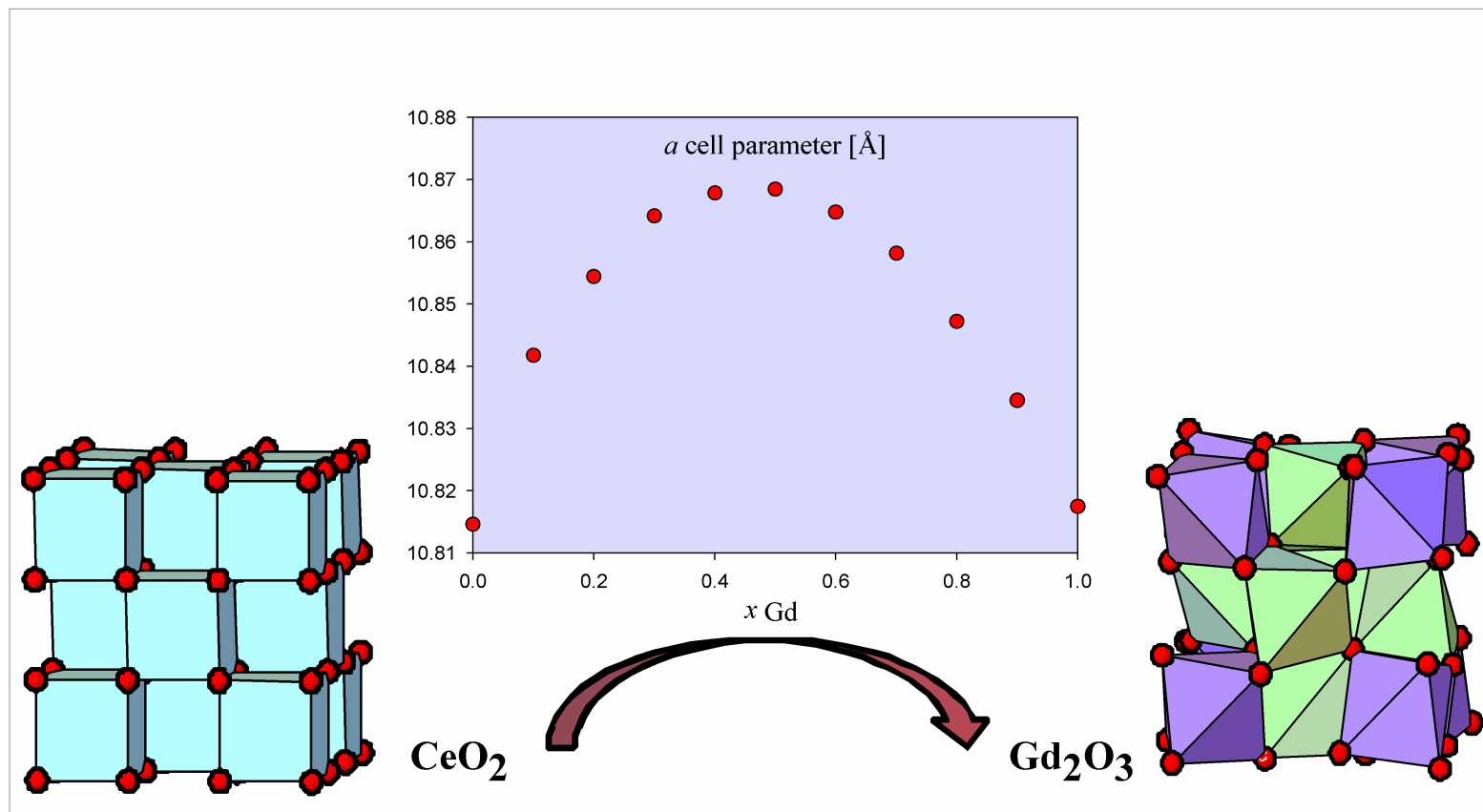
Structure refinement (mixed system)





Structure refinement



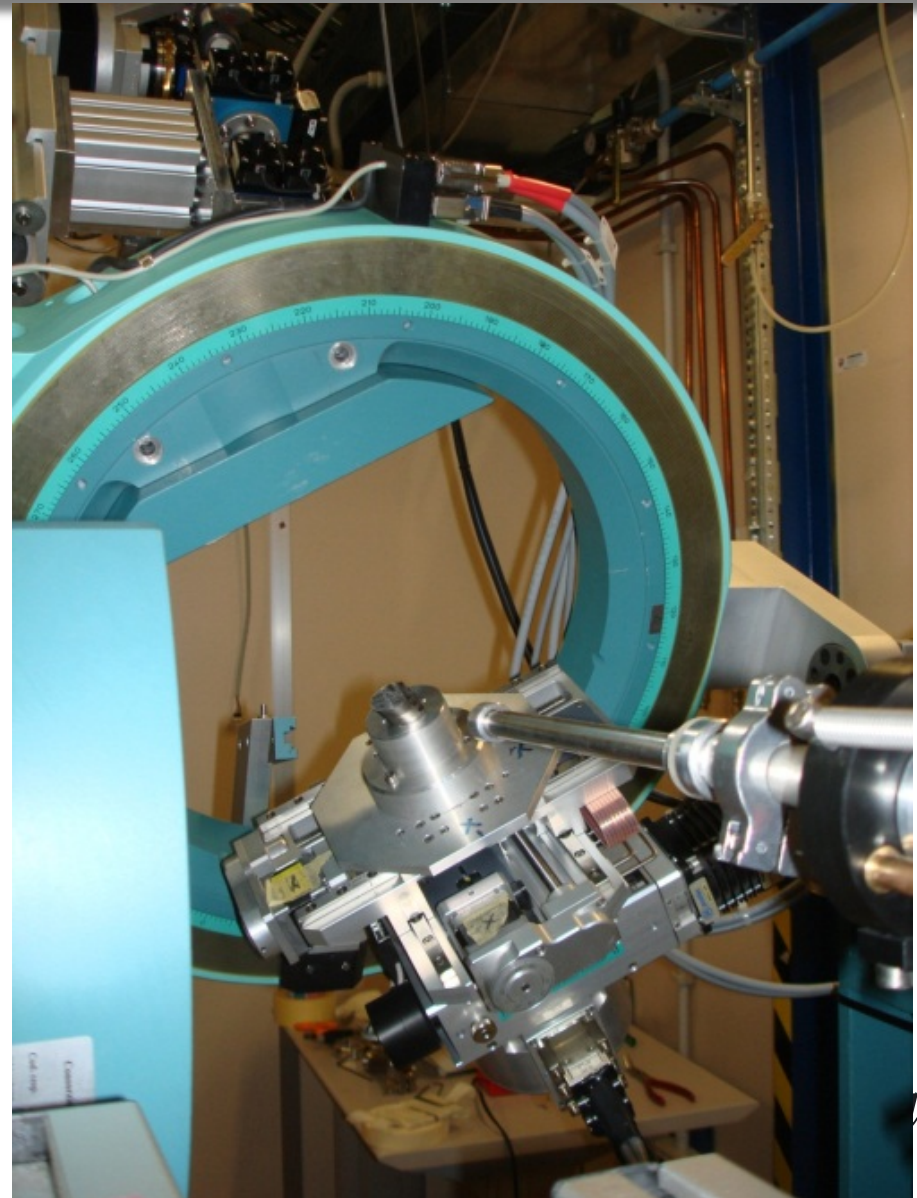


Journal of Solid State Chemistry 190, 24(2012)



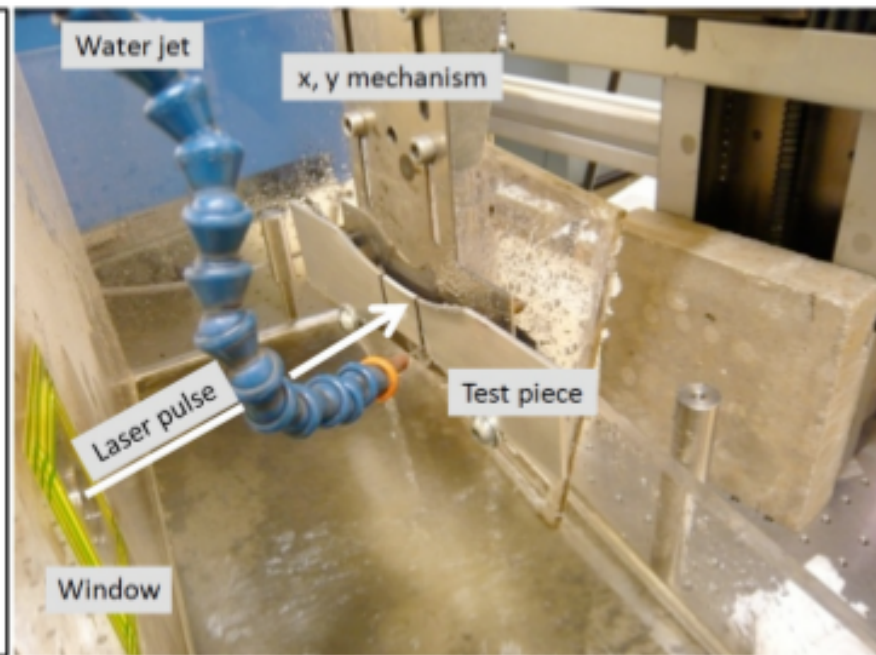
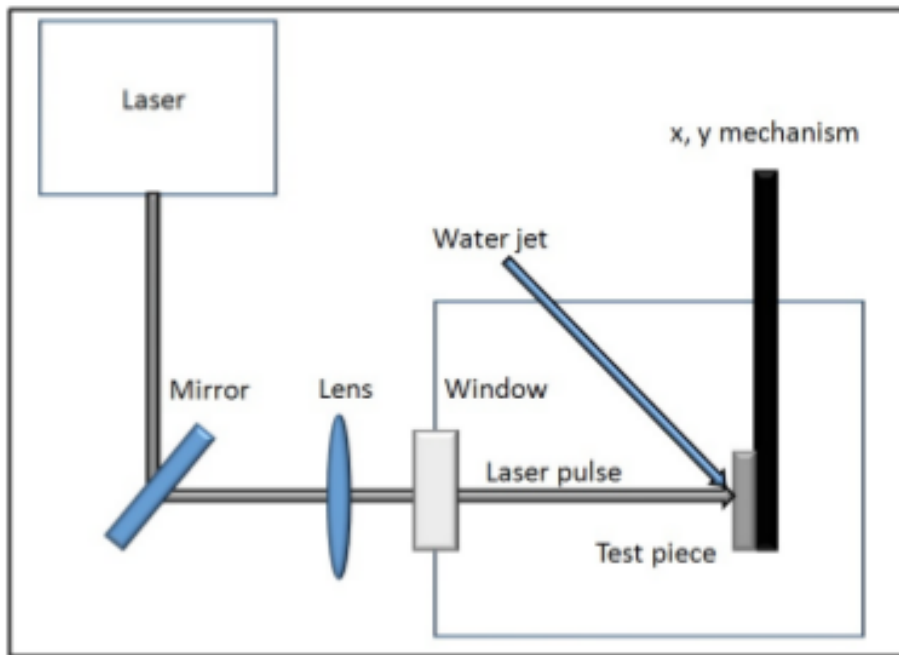
Residual stress measurements

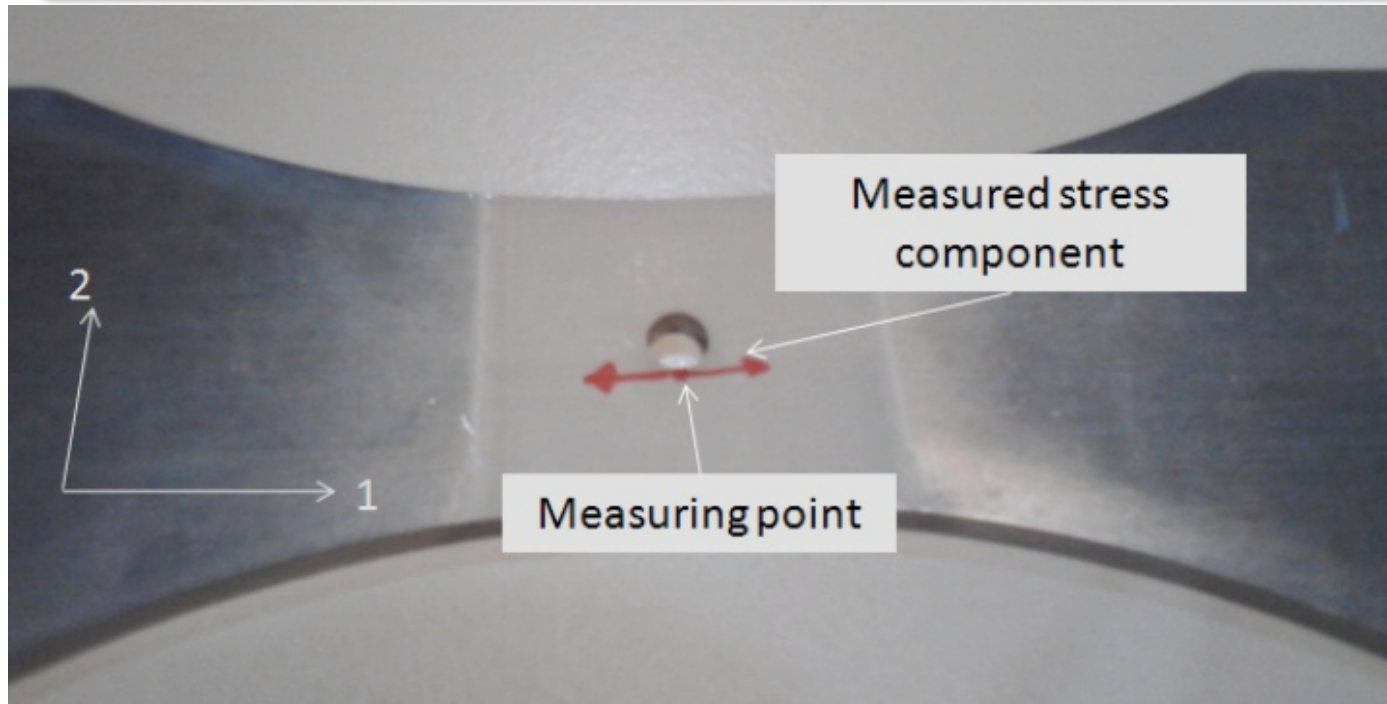
- Stress inside the crystal lattice
- Measurement of shift of diffraction peak under different angles
- Compressive stresses often induced on purpose to strengthen materials



- Laser Shock Peening (LSP) is a relatively recent technique used for the insertion of compressive residual stresses in metallic materials.
- LSP uses laser generated shock waves
- Locally, the laser creates a high pressure plasma
- As a consequence of the plastic deformation compressive residual stresses are established







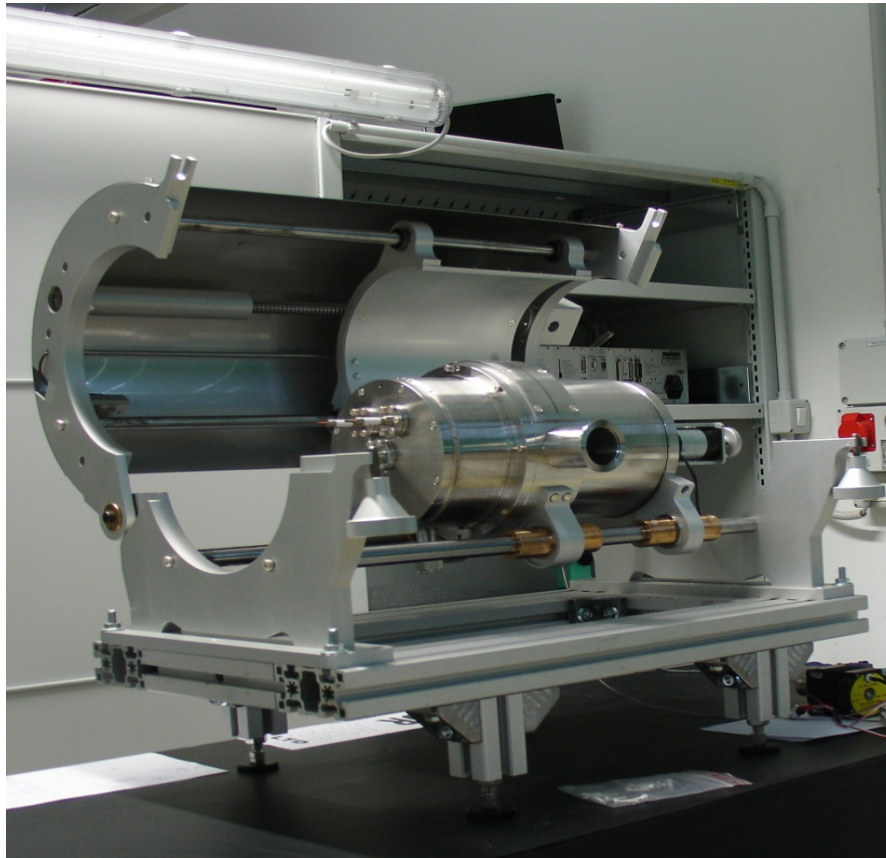
- Al based alloy 6082-T6
- Thin sheets typical of aircraft constructions
- Laser peening was applied around the hole before and after drilling



| Energy [keV] | Attenuation length [μm] | Residual stress hole before [MPa] | Residual stress hole after [MPa] |
|-----------------|---|--------------------------------------|-------------------------------------|
| 9 | 109 | -76.30 | -127.09 |
| 12 | 256 | -46.22 | -129.54 |
| 15 | 497 | -117.68 | -175.81 |



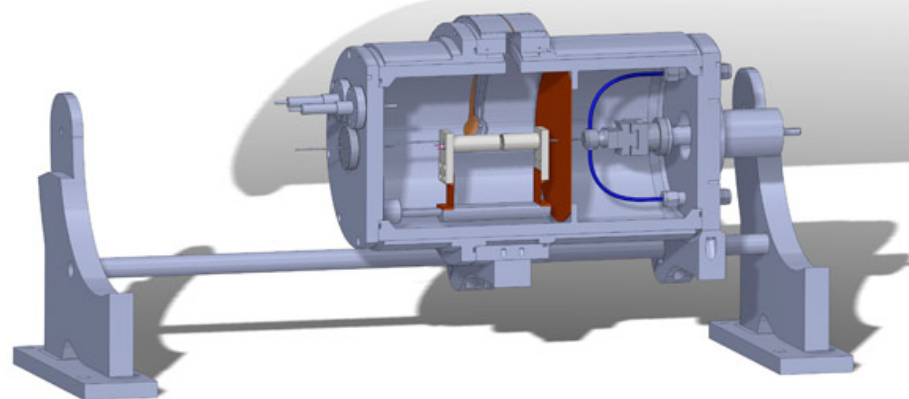
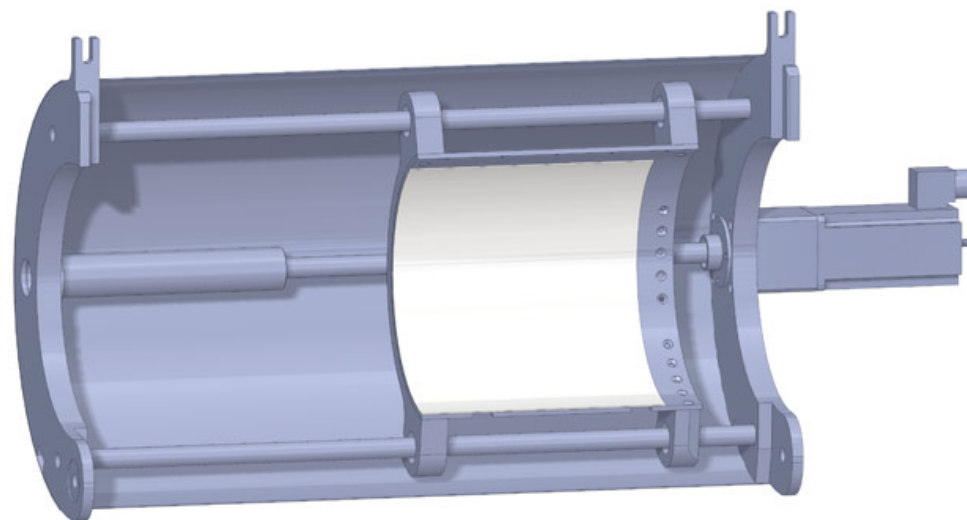
Phase transitions at high temperatures

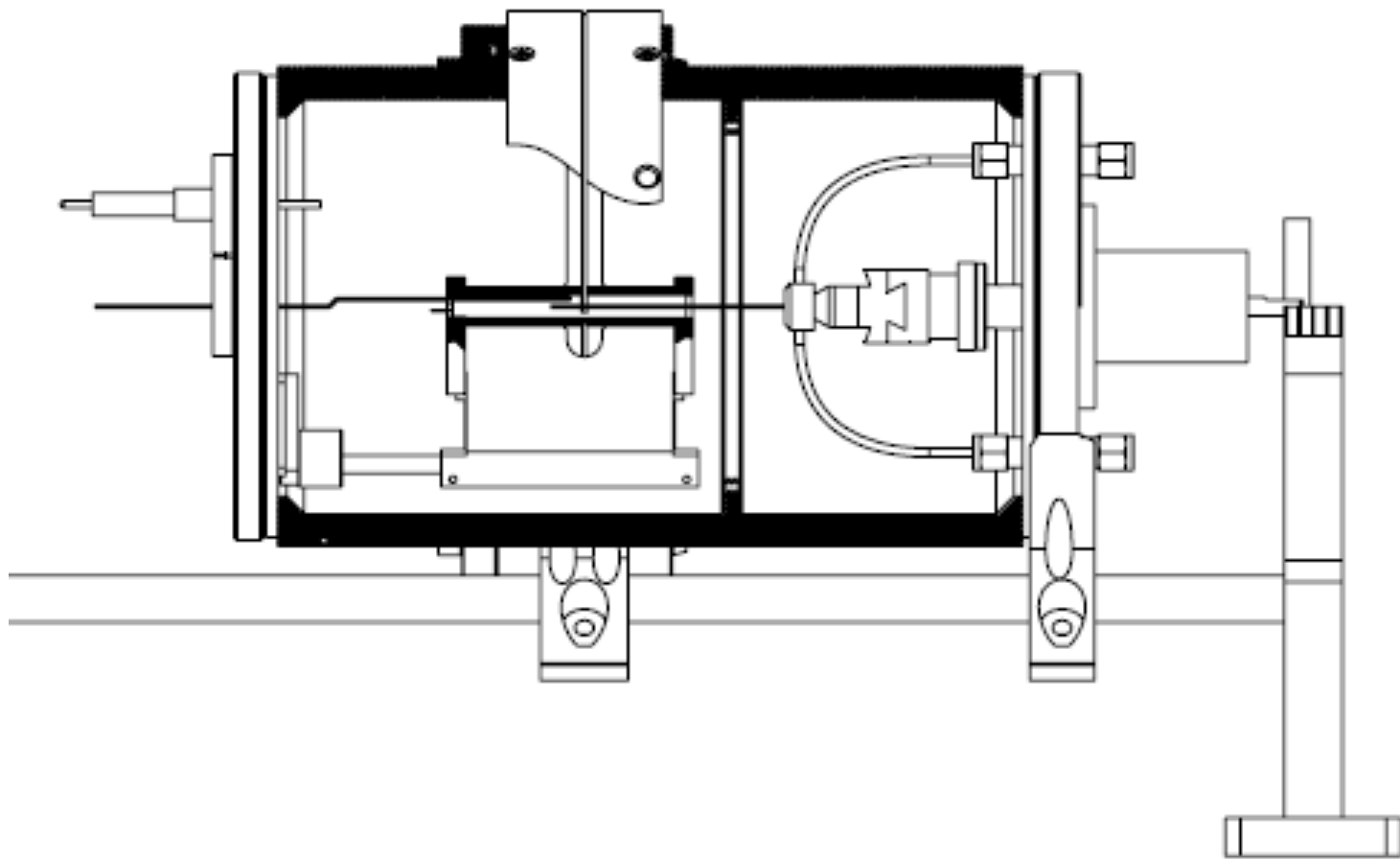


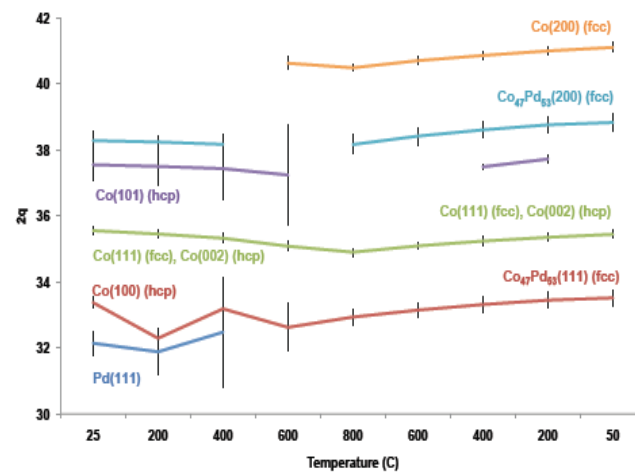
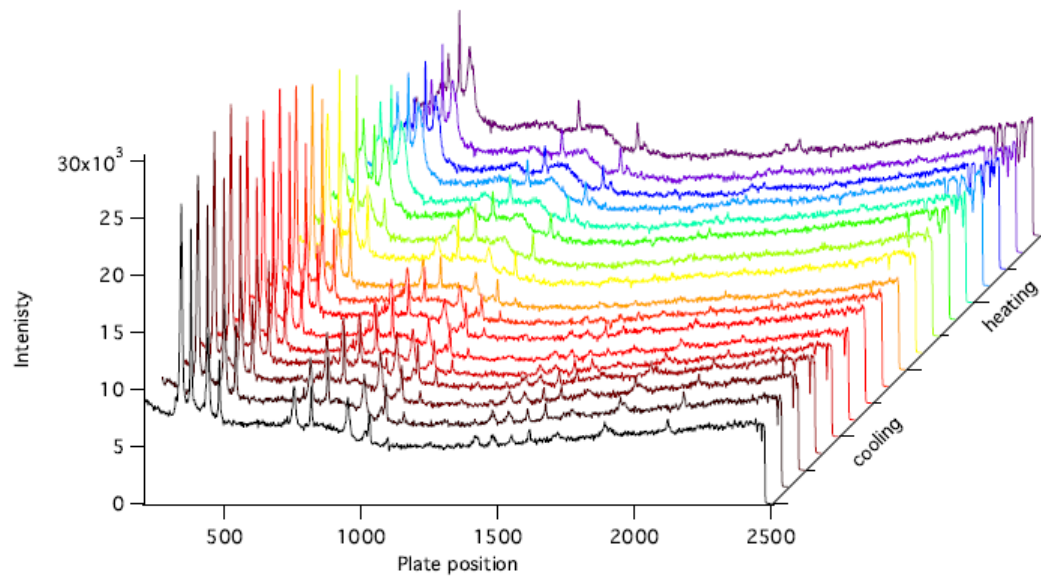
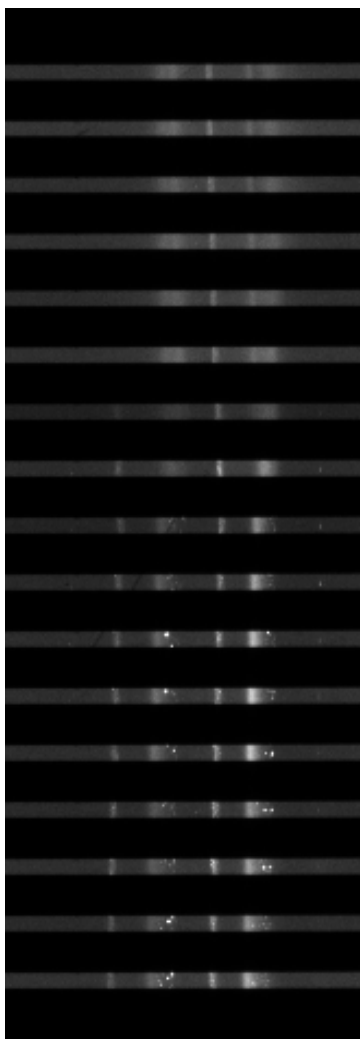
- Designed as a stand alone equipment
- Maximum temperatures reached in current setup 1100 C.
- Ideal for powder samples.
- Diffraction data recorded on a translating Imaging plate.
- Remote controlled
- Thermally isolated via water cooled shielding

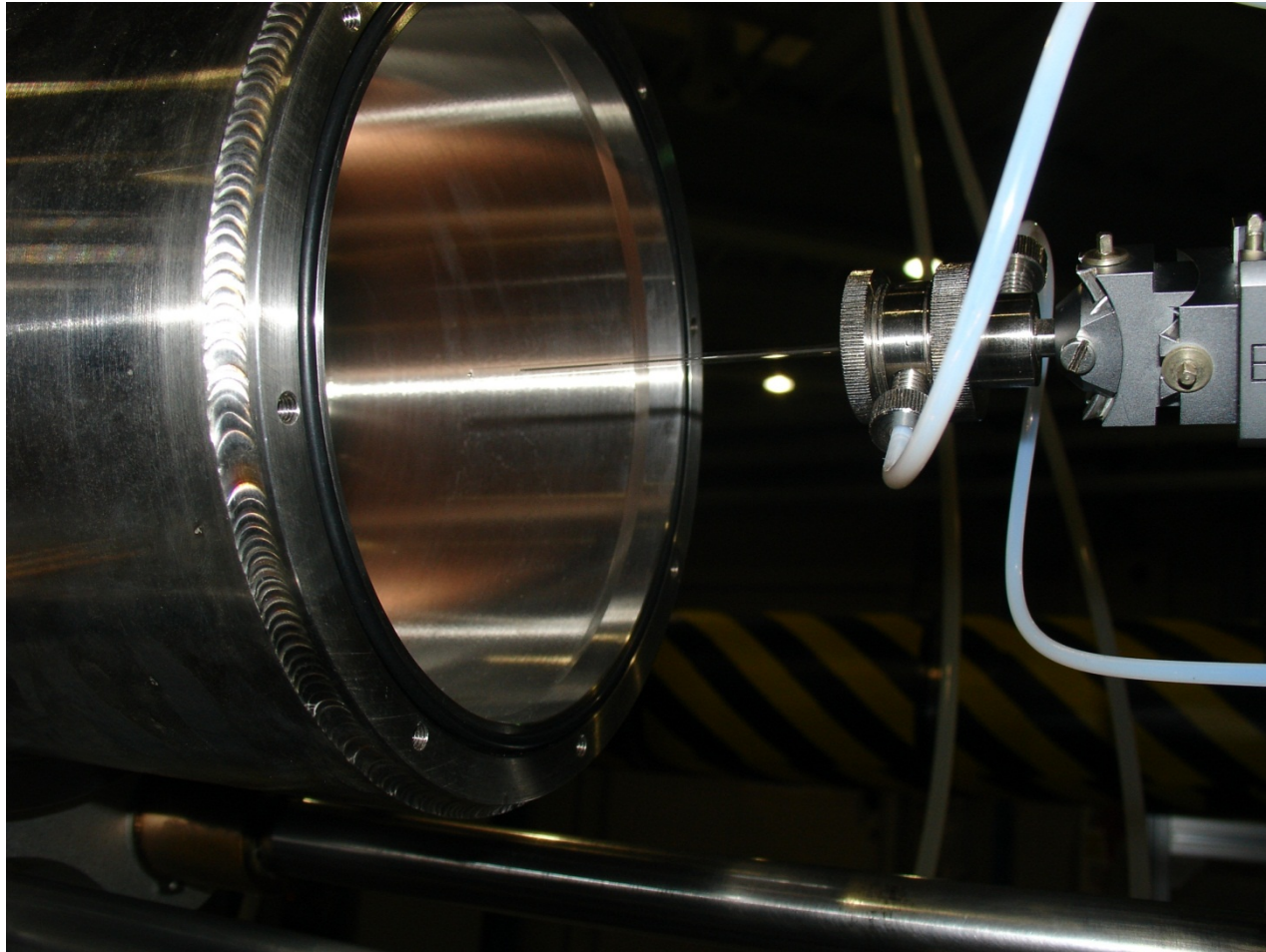
(Journal of Synchrotron radiation, accepted)



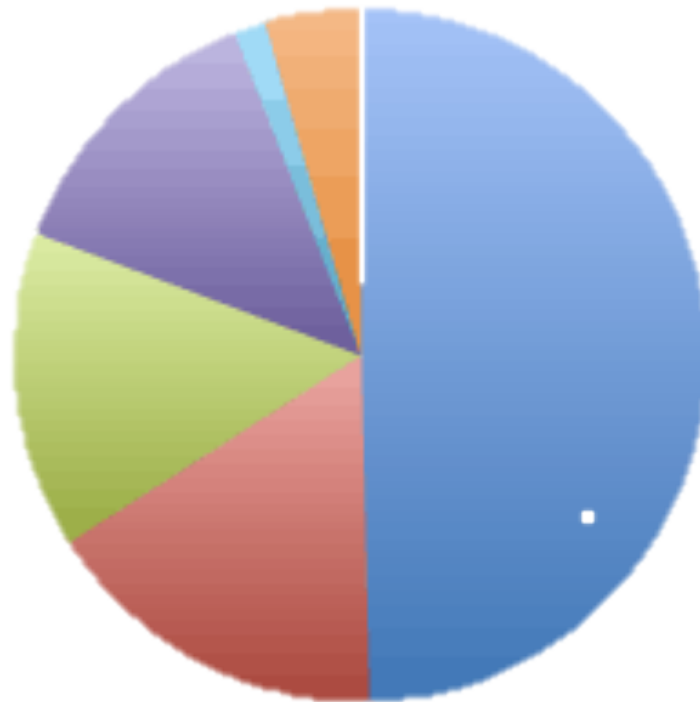




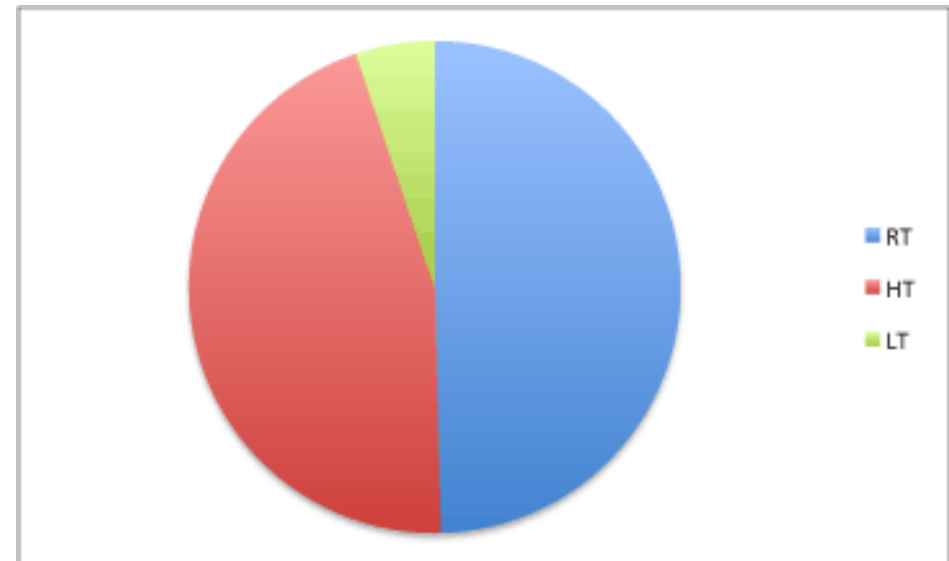




Sample form factors / temperature treatment



- CAPILLARY (67)
- FURNACE (22)
- STRAIN/TEXTURE (20)
- GRAZING (18)
- USER'S CELL (2)
- OTHER (6)



The MCX group

Andrea Lausi



Jasper Plaisier



Mahmoud Abd El-Latief



Giulio Zeraushek



Welcome!

UniVenice: P. Riello, A. Benedetti

UniTrento: M. Leoni, P. Scardi

